The Verwey transition—a new perspective

2004 J. Phys.: Condens. Matter 16 R145

(http://iopscience.iop.org/0953-8984/16/7/R01)

INSTITUTE OF PHYSICS PUBLISHING JOURNAL OF PHYSICS: CONDENSED MATTER

J. Phys.: Condens. Matter **16** (2004) R145–R178 PII: S0953-8984(04)69063-1

TOPICAL REVIEW

The Verwey transition—a new perspective

Joaquín García and Gloria Subías

Instituto de Ciencia de Materiales de Aragón, CSIC–Universidad de Zaragoza,
Plaza San Francisco s/n, 50009 Zaragoza, Spain

Received 15 September 2003, in final form 13 November 2003
Published 6 February 2004
Online at stacks.iop.org/JPhysCM/16/R145 (DOI: 10.1088/0953-8984/16/7/R01)

Abstract

This review puts in doubt the classical description of the Verwey (metal–insulator) transition in magnetite on the basis of the wide set of experiments carried out over the last 60 years. We re-analyse here the most relevant experiments used to study the Verwey transition from the point of view of their degree of agreement with the proposed Fe^{2+}–Fe^{3+} charge ordering model. We will consider three groups of experimental studies, according to their capability of detecting different ionic species and/or a charge periodicity: (1) Experiments which have been interpreted using the charge ordering model as the starting point though they are not able to demonstrate its validity. This is the case for macroscopic properties such as the electrical resistivity, the heat capacity and the magnetic properties. (2) Experiments which can distinguish different types of Fe ions, such as Mössbauer, nuclear magnetic resonance (NMR) and electronic spectroscopies. However, we show that they are not able to associate them with a specific valence (2+ or 3+ in our case) and, in some cases, they observe more than two different kinds of iron atoms. (3) Diffraction (x-ray, neutron and electron) experiments, which are the most conclusive ones for determining a periodic ordering of different entities. These experiments, instead, point to the lack of ionic charge ordering. We will focus, in particular, on the discussion of the results of some recent x-ray resonant scattering experiments carried out on magnetite that directly prove the lack of ionic charge ordering in such mixed valence oxide. Furthermore, we also reconsider some so-called Verwey-type transition metal oxides in terms of the applicability of the Verwey charge ordering model. We show that a complete charge disproportionation (δ) is not experimentally observed in any of these compounds, the maximum δ being less than 0.5 e^-. Regarding the theoretical framework, we will outline some relevant implications for the description of the physics of 3d transition metal oxides of this critical re-examination of the experimental facts on magnetite. Electronic localization should then occur involving more than one transition metal atom, so the definition of ionic d states loses its meaning in mixed valence transition metal oxides.

Contents

1. Introduction

Magnetite is the magnetic material that has been known of for the longest time. It was discovered 2500 years ago by Thales of Miletus (625–547 BC). Its 'magic' properties have been a matter of speculation throughout history. Transition metal (TM) oxides and, in particular, magnetite have been taken as a starting model for an important part of present-day solid state physics [1–8]. For instance, the present knowledge of magnetism is mainly based on studies carried out on magnetite. It is needless to recall that magnetite provided one of the first examples of the application of Néel's two-sublattice model of ferrimagnetism [9].

Apart from the magnetic properties, the other relevant phenomenon is the occurrence of a structural transition at around 120 K. This phase transition is called the Verwey transition as Verwey was the first to report on it in 1939 [10–12]. At this phase transition, a decrease of two orders of magnitude in the electrical conductivity occurs in such a way that at low temperatures magnetite is an insulator and above the Verwey transition temperature it is a metallic conductor. Verwey explained the change in conductivity as due to charge localization on the octahedral iron sites, Fe^{3+} and Fe^{2+} ions ordering periodically in the crystallographic lattice. In spite of this long period of investigation, this transition is still a matter of discussion. However, most of the metal–insulator transitions of mixed valence compounds are classified as Verwey type assuming that some kind of charge ordering (CO), i.e., ordering of the ionic charge state, occurs [13]. The interpretation given by Verwey has persisted to this day, in spite of the fact that after more than 60 years from the discovery of the transition it has proved impossible to achieve a consensus on the specific ionic ordering. Recently, with the aim of precisely determining the ionic ordering in magnetite, we have carried out x-ray resonant scattering experiments at the Fe K edge at the (002) and (006) forbidden reflections above and below the Verwey transition [14, 15]. Although our results do not completely disallow the occurrence of some kind of charge density wave with high periodicity, they establish that none of the charge ordering models which satisfy the Anderson condition [16] are compatible with our experiment, including the Verwey model. Several reviews have been published previously [2–8]; the recent one by Walz specifically criticizes our x-ray scattering results in a negative and superficial way. In this review, we will refute all the arguments advanced by that author and we will show that there is no experimental proof of the existence of Fe^{3+}–Fe^{2+} charge ordering. On the contrary, many experiments show the lack of such ordering in magnetite. We pinpoint this review as critical reading due to the fact that the acceptance of the absence of ionic charge ordering in magnetite is an important point that could help in revising the generally accepted hypothesis of the ionic model for transition metal oxides.

We will place emphasis on the discussion of the structure, magnetic ordering and microscopic experiments which tried to demonstrate the existence of ionic charge ordering. We will distinguish between techniques able to demonstrate the existence of such charge ordering and experiments which are interpreted taking the charge ordering model as a hypothesis but do not demonstrate its existence. In section 2, we will review the main points related to the description of the metal–insulator transition of magnetite in terms of the classical Verwey CO model. Section 3 will be devoted to reviewing the three types of experimental techniques (macroscopic property, spectroscopic and electronic techniques, and diffraction techniques) extensively used as proofs of the occurrence of CO in magnetite. We re-examine them one by one, showing the degree of agreement with the CO model, i.e. up to which limit they can be considered as a proof of the existence of a periodic ordering of ions. Related mixed valence transition metal oxides which present metal–insulator transitions also classified as CO type are also briefly reviewed in section 4. We will show that none of these compounds can be described in terms of ionic charge ordering and that a different degree of charge disproportionation exists depending on the particular compound, which demonstrates the absence of such ionic ordering. Finally, we will outline some implications for the theoretical description of TM oxides derived from the absence of ionic charge ordering in magnetite (and in other mixed valence TM oxides). Conclusions in terms of the present knowledge of solid state physics are given at the end.

2. The Verwey transition: a classical description

Magnetite belongs to the spinel ferrite materials group. The spinel crystal structure was first reported for magnetite by Bragg [17, 18]. The ideal spinel structure consists of a cubic close packing of the oxygen ions with, in between, a large number of holes, which are partially filled with the metal ions. The structure is cubic, space group $Fd\bar{3}m$. The general chemical formula can be written as $Fe^{3+}[Fe^{2+}, Fe^{3+}]O_4$ from the ionic point of view. Here, octahedral iron ions are indicated between brackets (16d B site) and the tetrahedral iron ions before the brackets (8a A site); see figure 1. According to this formula, Fe^{2+} and Fe^{3+} ions coexist at the same crystallographic site in the so-called inverse spinel structure. Below $T_N = 860$ K, magnetite orders ferrimagnetically [9]. The magnetic ordering, typical of Néel's two-sublattice model, implies that the tetrahedral (A) and octahedral (B) metal ions are aligned ferromagnetically within each sublattice and antiferromagnetically between the two sublattices. This magnetic structure agrees with the saturation magnetic moment, 4 μ_B, determined experimentally [19] and it was one of the first proofs of the validity of the Néel ferrimagnetic model, latter confirmed by means of neutron diffraction. In fact, the saturation magnetic moment corresponds to $\mu(Fe^{3+}B) + \mu(Fe^{2+}B) - \mu(Fe^{3+}A)$. As we will show later, even if this expression agrees with the ionic model, detailed neutron scattering experiments [20] have shown that the individual magnetic moments do not correspond to the ionic ones.

Magnetite undergoes a phase transition at $T_V \sim 120$ K. This transition was first detected by means of heat capacity measurements by Parks and Kelley [21] in 1926. But the greatest interest in this transition was aroused when Verwey found that the transition is accompanied by a strong discontinuity in the electrical conductivity. Verwey characterized it as an order–disorder transition and he proposed an ionic model to explain the strong change in the electrical transport properties [10–12]. The model can be viewed as follows: above T_V, Fe^{3+} and Fe^{2+} are dynamically disordered in the lattice. The dynamical transformation of Fe^{2+} into Fe^{3+} implies motion of the electron to be responsible for the metallic conductivity above T_V. For below T_V, Verwey proposed a long range spatial ordering of the Fe^{3+} and Fe^{2+} ions. This periodic order localizes the electron, preventing the motion of carriers. This simple model was very successful in giving a reasonable interpretation of the electrical resistivity measurements [10, 22] and it

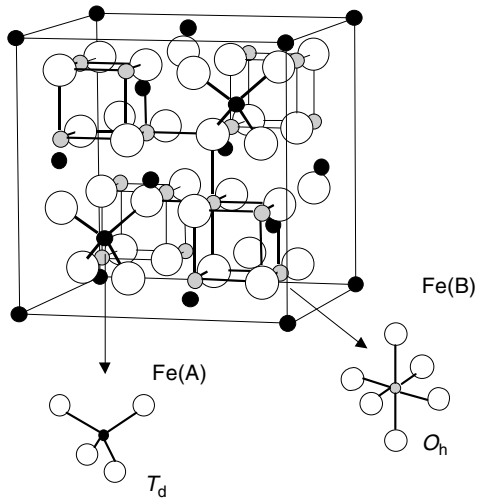

Figure 1. The crystal structure of spinel Fe_3O_4, ideally described as the cubic closest packing of oxygen atoms. A large ball shows an oxygen ion, a small dark ball denotes an A site (tetrahedral) iron ion and a small light ball denotes a B site (octahedral) iron ion.

has been applied to a lot of new phase transitions, of so-called Verwey type. In our opinion, this fact, combined with the simplicity of the model, has been the reason that this model has survived for nearly 60 years. Verwey proposed a specific scheme of ordering of the Fe^{3+} and Fe^{2+} octahedral ions as shown in figure 2. Within this model, the charge ordering will produce a structural phase transition from the cubic to an orthorhombic phase, where Fe^{3+} and Fe^{2+} ions occupy alternately the (001) planes forming channels of homovalent ions along the directions [110] and [$\bar{1}$10]. This ionic ordering should induce the appearance of the (002) reflection, forbidden by symmetry in the high temperature phase. The ordering proposed by Verwey was apparently confirmed by neutron diffraction experiments performed by Hamilton in 1958 [23]. This observation was the experimental support of the Verwey model, considered by the scientific community as a milestone in the physics of transition metal oxides. This belief, combined with the difficulties in explaining the insulator state of transition metal oxides (in particular, NiO) in the framework of the band theory, was the origin of Mott's theory of metal–insulator phase transitions [24]. Simultaneously, numerous experiments were performed on magnetite, some of them trying to confirm the charge ordering scheme proposed by Verwey or, at least, the existence of two different ionic states in the low temperature phase of magnetite. None of them were able to rigorously prove either of the two hypotheses.

Other experiments, for instance resistivity measurements, took the Verwey model as a hypothesis to explain their experimental results but, despite very nice agreement, they do not demonstrate the Verwey type of ionic ordering. The situation should have changed after the neutron diffraction experiments of Shirane *et al* [25], which demonstrated that the (002) forbidden reflection observed by Hamilton was, in reality, a spurious signal coming from multiple scattering. Later on, the structural determination of the low temperature phase by Iizumi *et al* [26] directly contradicted the Verwey model. This precise and rigorous structural determination shows two important points: first, the octahedral Fe–O interatomic distances determined are far from the ones expected for Fe^{3+} and Fe^{2+} octahedral ions. We transcribe a sentence of Iizumi's paper: '*The Fe–O distances are indicated in figure 5 (Pmca model). The displacement pattern in both space groups is complex, and there is no significant variation*

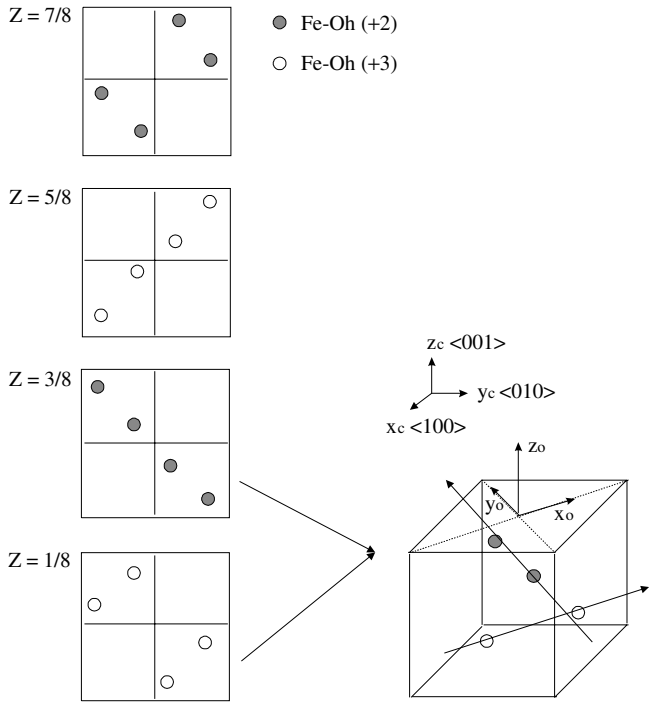

Figure 2. An illustration of the ordering of Fe^{2+} and Fe^{3+} octahedral B ions along the $\langle \bar{1}10 \rangle$ and $\langle 110 \rangle$ directions, as proposed by Verwey [10, 11]. Inset: a schematic representation of one octant of the spinel structure showing the octahedral Fe ions. (x_0, y_0, z_0) axes refer to the orthorhombic low temperature unit cell.

in the mean Fe–O distances for the octahedral sites, such as might be accompany charge ordering.'

Second, at least four different octahedral iron sites are distinguishable in the low temperature phase. (The authors believed that the real symmetry is Cc with 16 different octahedral iron sites.) It is obvious that the number of different octahedral sites is different from a bimodal distribution, i.e. only two different atoms. These important points seem to have been forgotten in the scientific discussion. Perhaps the conference in Cambridge (1979) arranged by Sir Nevill Mott with the 'the Verwey transition' as its topic obscured the relevant results obtained from this experiment. Despite these 'negative results', the scientific community has not discarded the Verwey model, the actual situation in science being the following: everybody assumes that the Verwey transition originates from ionic localization of the carrier, giving rise to a periodic ordering of Fe^{3+} and Fe^{2+} ions, even if the detailed scheme ordering is still unknown.

3. Charge ordering in magnetite: reconsideration of the experimental studies

Prior to focusing on the different experimental techniques used to demonstrate the occurrence of charge ordering in Fe_3O_4 we would like to review the concept of 'charge ordering' itself. Classically, as is shown in most of the textbooks, charge ordering is defined as a periodic arrangement of ions with different integral valence states [4, 8]. Nowadays, this concept seems to be relaxed. Some authors implicitly assume that the ions (Fe^{3+} and Fe^{2+} in our case)

cannot be considered equivalent to those in the pure compounds (Fe_2O_3 and FeO). Thus the observation of two physical features has been considered as a proof of identification of two ions with different integral valence states. In any case, even in this situation, only two different ions should be identified. We will discuss these two points for the case of magnetite in the following sections.

A large number of experimental techniques have been applied to characterize the charge ordering phenomena in Fe_3O_4:

(i) Experiments mainly devoted to measuring macroscopic properties such as the electrical resistivity, heat capacity, magnetization and magnetic after-effect. Such measurements have been interpreted using the Verwey model as a hypothesis. The Verwey model nicely reproduces the experimental data, but these techniques are unable to discriminate between the Fe ions and to determine the model of ordering. In other words, the interpretation of the experimental facts is correct if the charge ordering model is.
(ii) Other experiments, for instance Mössbauer, NMR and electronic spectroscopies, are able to distinguish different kinds of ions but they cannot say anything about the model of ordering.
(iii) The third group of experiments comprises those able to determine the crystallographic scheme of ordering of the two entities. These experiments are the most conclusive. In fact, they can distinguish two different kinds of ions and determine their scheme of ordering. Clearly, diffraction is the most suitable technique for determining a periodic order (x-ray, neutron or electron diffraction). However, the determination of different crystallographic sites for the atoms in the lattice does not necessarily mean that they are associated with atoms with different integral valence states. As an example, the crystallographic structure of the hard magnetic material $Nd_2Fe_{14}B$ is described in terms of six different iron sites [27]. This does not imply the ordering of different ionic states.

The tunability of the synchrotron radiation has allowed us to develop new x-ray diffraction techniques. X-ray anomalous diffraction permits us to investigate the energy dependence of the anomalous part of the atomic scattering factor using energies of the incident photon in the neighbourhood of an atomic absorption edge. This technique consists in recording the intensity of a Bragg reflection as a function of the energy of the scattered photons crossing an atomic absorption edge. Due to the fact that the energies of the absorption edges are specific to an atom and an electronic level, x-ray anomalous diffraction has all the capabilities of diffraction and x-ray absorption in a single technique. It provides short range order information about the set of long range ordered atoms selected by the diffraction condition and it is chemically, valence and site specific. This technique is known as DAFS (diffraction anomalous fine structure) [28, 29]. X-ray resonant scattering is an x-ray anomalous diffraction technique, where the reflections investigated are either Thompson forbidden or very low intensity ones (satellites). The main contribution to the x-ray structure factor for these reflections comes from the anomalous part of the atomic scattering factor of a specific atom (selected by the photon energy of its absorption edge). As the structure factor for forbidden (or almost forbidden) reflections is given by the difference of atomic scattering factors of particular atoms in the lattice, the intensity of this reflection appears (or it is highly enhanced) only at definite photon energies (so-called resonances) where the contrast of the anomalous part of the scattering factor is maximum. The atomic anomalous scattering factor is intimately correlated with the x-ray absorption coefficient and for dipolar transitions is a two-range tensor. Thus, resonance can be observed as arising from differences among the terms of the scattering tensor or from a different orientation of this tensor in the lattice (ATS, anisotropic tensor scattering reflections). In the first case, the absorption edges (or the anomalous scattering factors) of atoms with different

valence states are shifted (chemical shift) in energy. Consequently, a strong resonance at the absorption edge must be observed for sequences of the charge with the periodicity of the reflection studied in the crystal. The appearance of a resonance at the absorption edge does not guarantee the occurrence of charge ordering, as ATS reflections can also give rise to the same kind of resonance. In this second case, the intensity of the ATS reflections depends on the x-ray polarization and azimuthal angle of the diffraction plane. Thus the azimuthal and the polarization behaviour of the x-ray resonant scattering reflection permits us to discriminate between ATS and charge ordering reflections. A complete survey of x-ray anomalous diffraction and x-ray resonant scattering techniques is given in [30].

3.1. Macroscopic properties

Transport and magnetic properties, the specific heat and thermodynamic properties of magnetite across the Verwey transition have been extensively reported [5, 31, 32]. Here we will discuss how far experiments probe the model of ionic localization.

3.1.1. Electrical resistivity. The fingerprint of the Verwey transition is the discontinuous change of the electrical resistivity at T_V, this being one of the first examples found of a metallic–insulator phase transition. The interpretation given by Verwey in terms of ionic ordering was very successful and it was responsible for the extension of this model to other intermediate valence oxides, which show metal–insulator phase transitions [3–6]. The electrical conductivity of magnetite has been measured by several authors [10, 22, 31–36], all of them indicating a sharp discontinuity at the phase transition (see figure 3). The proposed two-state order–disorder model has also been very successful in accounting for the electrical characteristics of magnetite [31], although we would like to remark that the assignment of the two-state system to Fe^{3+} and Fe^{2+} octahedral ions itself implies a correlation among the octahedral iron ions in pairs. Another characteristic of the Verwey transition is the strong dependence of the resistivity discontinuity at T_V on the oxygen stoichiometry (iron defectivity) or doping substitutions. A careful study of this dependence has been carried out by Honig and co-workers, showing the existence of two regimes of the Verwey transition depending on the iron defectivity (δ) [31, 37–40]. For $\delta < \delta_c$, $\delta_c = 0.0117$, $Fe_{3-\delta}O_4$ exhibits a first-order phase transition, being of second order for $\delta > \delta_c$. For $\delta > 3\delta_c$, the transition disappears [37, 38] with δ_c corresponding to a deficiency of one electron out of the 96 cations of the low temperature base-centred monoclinic cell ($2\sqrt{a}, 2\sqrt{a}, 2a$), a being the spinel cubic unit cell parameter. If we consider the vacancy to be located at the octahedral sites, one out of 64 ions breaks the long range ordering. The interpretation of these results has been made in terms of percolation theory, and is very successful in reproducing the occurrence of long or short range ordering, although this calculation was only based on the experimental fact that the low temperature structure is the Cc one. However, the tolerance in composition (i.e., the deviation of the $Fe^{3+}/Fe^{2+} = 1$ ratio) is larger than 1.5% for order–disorder phase transitions. Moreover, the percolation limit for a spin $= 1/2$ Ising lattice is also considerably larger than the experimental limit found for magnetite (as a first approximation we can consider each octahedral iron as a spin $1/2$ which can have the two states +3 and +2). Thus, the very small stoichiometric tolerance in magnetite indicates that the conformation of the low temperature electronic structure is highly dependent on the electronic filling, and this is very difficult to reconcile with an ordering of two independent entities.

The existence of metallic conductivity above T_V in magnetite in comparison with spinel ferrites such as $CoFe_2O_4$, $MnFe_2O_4$ and $NiFe_2O_4$ being insulators indicates that the existence of a mixed valence state on B sites is responsible for the electrical conduction. This observation

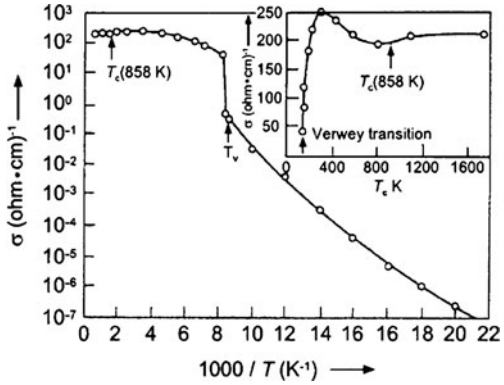

Figure 3. The temperature dependence of the electrical conductivity of Fe_3O_4. From [36].

is correct although it does not mean that the fluctuating ionic model is valid. The mechanisms proposed to explain the electrical conductivity in magnetite follow Mott's view of the Verwey transition, i.e. a phase transition from a Wigner glass into a Wigner crystal. The low temperature conductivity for Fe_3O_4 has been explained in terms of various mechanisms, from tunnelling of electrons to multiple variable-range hoppings of small polarons. We will deal here not with the various models proposed to explain the conductivity in magnetite and ferrites (excellent reviews of this topic are given by Brabers [5] and Tsuda [3]), but with their implications for the ionic localization model. First, a lot of interpretations have been given in terms of the ionic model though the conduction mechanisms seem to change with composition. As an example, the conduction in $Ni_xFe_{3-x}O_4$ [41, 42] has been described as due to nearest neighbour and variable-range hopping for high nickel concentrations, whereas the formation of a Coulomb gap seems to take place for lower concentrations. Another example that shows that the mechanisms for electrical conduction in magnetite do not correlate with the ionic model is the fact that the conduction mechanism for Verwey-type compounds such as $REFe_2O_4$ is very different compared to that of magnetite [43]. Moreover, the Verwey transition disappears in YFe_2O_4 on applying a hydrostatic pressure, indicating that the sensitivity of this transition to the interatomic distances is stronger than in Fe_3O_4 where T_V slightly shifts to lower temperature [5]. As a final remark, for Fe_3O_4, the effect of residual stresses lowering T_V, broadening the temperature width of the anomalous specific heat at the phase transition and decreasing the discontinuous conductivity change at T_V cannot be explained with a model as naive as the charge ordering model [34].

3.1.2. Heat capacity. Heat capacity measurements show an anomaly at the Verwey transition temperature, which is highly dependent on the stoichiometry and the residual stress [34, 38, 44]. The relevant magnitude that can give us information about the mechanism of the phase transition is the entropy change of the transition, ΔS_V. The experimental molar entropy content of this transition approaches the value of $\Delta S_V = R \ln 2$ instead of $2R \ln 2$ expected from a model of order–disorder phase transitions where the Verwey transition is caused by the ordering of a binary random mixture of Fe^{2+}–Fe^{3+} ions on the B sites. Several attempts have been made to resolve this discrepancy. Honig, Aragón and Shepherd [31, 39, 44], using the two-state model of Kittel, found a configurational entropy of $R \ln 2$, but this result is implicitly contained in their model, as it uses a couple of octahedral Fe ions with two possible configurations, Fe^{3+}–Fe^{2+}

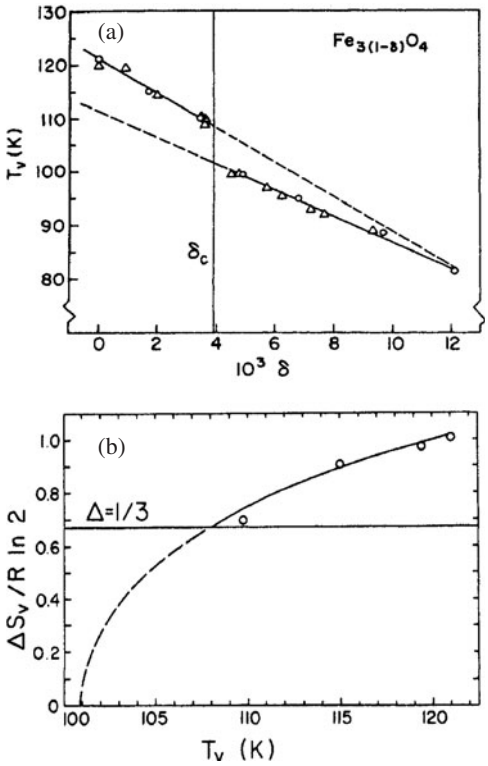

Figure 4. (a) The dependence of the Verwey transition temperature T_V on the stoichiometry parameter δ in $Fe_{3(1-\delta)}O_4$. Circles relate to calorimetric measurements and triangles to magnetic measurements. From [44]. (b) The entropy content of the first-order Verwey transition ΔS_V versus T_V for non-stoichiometric magnetite samples ($0 \leqslant \delta < 0.004$). The solid curve $\Delta = 1/3$ indicates the entropy content at the critical value δ_c. From [44].

and vice versa. It is obvious that this model is similar to a spin $= 1/2$ Ising model for each pair of octahedral irons so they found a configurational entropy of $R \ln 2$. Anyway, apart from the fact that this model artificially introduces a very strong constraint, it cannot explain the variation of entropy content as a function of the oxygen stoichiometry. The entropy content as a function of δ (iron defectivity) should be nearly constant in a strict order–disorder model, contrary to the experimental results. For illustration, figure 4(a) shows the variation of the Verwey transition temperature as a function of the iron defectivity whereas figure 4(b) reports the dependence of the entropy content, ΔS_V, on T_V [44]. The lack of agreement between the experimental and the theoretical estimates of ΔS_V could be explained as due to the existence of short range order above T_V, but Shepherd *et al* [44] did not find any evidence for short range order in their heat capacity measurements.

3.1.3. Magnetic properties. Magnetite is a well-known ferrimagnet, archetypical of the spinel ferrites. The magnetic ordering in magnetite provided one of the first examples of the application of Néel's two-sublattice model. In this model, it is assumed that the magnetic interaction between the octahedral (B) and tetrahedral (A) iron ions is strongly negative and that between the ions of the same lattice is weak and positive. These interactions

favour an antiparallel arrangement of the sublattices A and B, the so-called collinear Néel configuration, and consequently the resultant magnetization is the difference between the A and B lattice magnetizations. Following the ionic model, the magnetic moments of A (Fe^{3+}) and B (Fe^{3+}/Fe^{2+}) sites are $\mu(A) = 5\ \mu_B$ and $\mu(B) = 9/2\ \mu_B$, respectively, so the net magnetic moment should be $4\ \mu_B$/fu. The experimental value determined by Weiss and Forrer is $4.07\ \mu_B$ [19]. The good agreement between the theoretical magnetization predicted by the simple ionic model and the experimental value was considered as a proof of the validity of this model. However, neutron scattering experiments [20] have demonstrated that the magnetic moment of the A site is very different from the expected theoretical value and the same applies to the B site magnetic moment. This means that the assumed cation distribution of Fe^{3+}/Fe^{3+}–Fe^{2+} among the T_d and O_h sites, respectively, is wrong in a strict sense. Moreover, below T_V no magnetic reflection was observed coming from the difference between the magnetic moments of the predicted ordered octahedral Fe^{3+}–Fe^{2+} ions. In fact, all the neutron scattering refinements made consider only one magnetic moment on the B octahedral site [26].

From the point of view of the magnetic interactions between sublattices, it is very difficult to reconcile the ionic charge ordering model with the proposed magnetic interactions responsible for the magnetic ordering. It is acknowledged that the magnetic ordering in oxide spinels is mainly due to superexchange interactions via the oxygen ions [5]. In the mean-field approximation, most of the models only used three interaction constants (J_{AA}, J_{BB} and J_{AB}) [9]. Some models distinguish between the two octahedral sublattices (Fe^{3+} and Fe^{2+}) increasing the number of exchange integrals [45]. However, it is well known that the mean-field approximation is a long range interaction and superexchange interaction is a short range interaction (nearest neighbour interaction). Thus, it is expected that, considering superexchange interactions, the dynamic disorder in the B sublattice above T_V should change the effective interactions and, consequently, a significant change must be observed in the magnetic properties at the Verwey transition. The saturation magnetic moment changes by less than 0.1% at T_V [33], demonstrating that the Verwey transition is not driven primarily by magnetic interactions and, correspondingly, that the metal–insulator transition has a minor effect on the magnetic properties. The hypothesis of a double-exchange mechanism as the origin of the coupling in the B sublattice does not improve the modelling of the thermal magnetization dependences [46]. Moreover, it would also imply a discontinuous change of the magnetic properties above and below T_V. In fact, the double-exchange mechanism should be suppressed in the low temperature Verwey phase.

The last property we would like to mention is the magnetic after-effect (MAE), as it has been claimed that MAE experiments on magnetite clearly indicate the existence of ionic states of different valence localized for at least several minutes [7, 47]. We are not expert in this technique, but it seems really hard to understand how a technique that measures the dynamics of the magnetic domain walls and their interaction with the lattice defects could give direct evidence of ionic ordering. In our opinion, the MAE data are interpreted on the basis of the ionic model but cannot be considered as a direct proof of the existence of charge ordering. In fact, Walz [7] explicitly says that the appearance of a characteristic MAE spectrum in the low temperature phase of Fe_3O_4 is a clear indication (not a demonstration) of electron localization.

Similar reasons can be given for other macroscopic properties such as thermal expansion, thermoelectricity and optical conductivity (see the books of Brabers [5] and Mott [24]). The experimental data are interpreted taking as reference the ionic model but, in all these cases, these macroscopic measurements cannot be considered as an experimental proof of charge ordering.

3.2. Spectroscopic techniques

3.2.1. Mössbauer and NMR techniques. Mössbauer and NMR techniques are able to distinguish ions with different ionic valence states or at different crystallographic sites but they cannot determine the ordering of these different species present in a sample. Dynamic aspects should also be observed in view of the typical probing time of these techniques, of the order of 10^{-8} s, which means that if the electron hopping between Fe ions occurs with a frequency $>10^{-8}$ s^{-1}, the ions see an average valence state.

The temperature dependence of the Mössbauer spectra shows only one spectral line above the Néel temperature, that Pan and Evans [48] fitted with two quadrupole doublets corresponding to the tetrahedral (A) and octahedral (B) sites. On the other hand, De Grave *et al* [49] described this high temperature spectrum as the sum of A site and B site doublets, consistently with the cubic symmetry on the A sites and the trigonal symmetry on the B sites. In the temperature range $T_V < T < T_N$, the spectrum consists of two superimposed six-line spectra corresponding to the A and B sites. The lines of the B site show a larger width and the respective hyperfine parameters are not typical for Fe^{3+} or for Fe^{2+}. This leads to the suggestion that the sixth electron jumps between adjacent Fe^{3+} and Fe^{2+} ions along the [110] B site chains with a frequency which is considerably higher than the inverse of the Mössbauer measuring time [50]. As a consequence, the Mössbauer effect cannot distinguish different valence states for the Fe at the B site [49]. Below T_V, an adequate model for the interpretation of the spectra has not been found yet, even if the transition is clearly reflected. Rubinstein and Forester [51] have interpreted the Mössbauer spectrum at low temperatures in terms of one A site spectral set and five magnetic components for the octahedral B sites. Recent studies [52] concluded, instead, that the Mössbauer spectrum below T_V is better fitted with only five components. Figure 5 shows the fit of the Mössbauer spectrum recorded at 4.2 K in zero applied field from a single crystal of Fe_3O_4 and the decomposition into five magnetic sextet components. One corresponds to the tetrahedral Fe A site and the other four are attributed by the authors to two non-equivalent octahedral Fe^{2+} and Fe^{3+} B sites [52]. We would like to emphasize here that the low temperature Mössbauer data are further evidence against the validity of the Verwey description that implies the existence of three components with the same intensity, one for each of the three kinds of atoms (tetrahedral Fe^{3+}, octahedral Fe^{2+} and octahedral Fe^{3+}).

NMR was the other technique extensively used as a proof of the existence of localized octahedral Fe^{2+} and Fe^{3+} since faster NMR relaxation is expected. This fact allows us to establish a correspondence between NMR lines and the valence of iron. Early experiments by Rubinstein and by Mizoguchi observed four types of resonance lines for the iron atom, one of them corresponding to tetrahedral iron and the other three to octahedral B irons [51, 53]. The lines corresponding to the tetrahedral A site are formed by four peaks of different widths and intensities, indicating the existence of more than four non-equivalent A sites in the unit cell. The spectrum corresponding to the octahedral iron is much more complex and at least five non-equivalent B sites among the 16 of the Cc unit cell were distinguished. Despite the fact that the number of sites was different to that expected from the Verwey charge ordering model, Mizoguchi sought to interpret the data maintaining the original idea of Verwey and proposing a new ordering pattern referred to as Mizoguchi ordering [53]. This ordering was not experimentally confirmed and consequently it was abandoned. Re-analysis and recent NMR experiments on magnetite below the Verwey temperature found 8 and 16 independent lines for tetrahedral and octahedral iron, respectively [54]. Figure 6 shows the temperature dependence of these NMR frequencies. This work showed that the NMR spectra are in accord with the Cc symmetry and the NMR relaxation results below T_V indicate that the states of

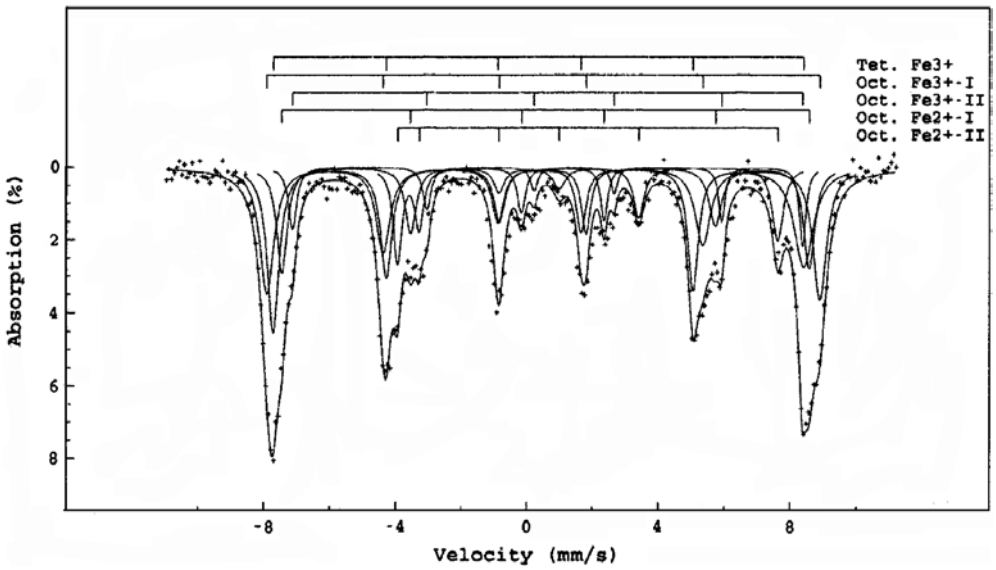

Figure 5. ^{57}Fe Mössbauer spectra recorded in zero applied field at 4.2 K from a single crystal of Fe_3O_4 cut perpendicular to the [111] axis. From [52].

iron ions on the B sublattice are so strongly mixed that the notion of 2+ or 3+ valence loses its meaning [54]. Mizoguchi obtained similar results in his recent NMR work. He identifies 16 non-equivalent octahedral B sites where the iron atoms show fractional valences or charge states ranging between 2+ and 3+. He proposes a charge density wave model but implicitly he demonstrates that neither octahedral Fe^{3+} nor Fe^{2+} can be identified on the B sites [55].

In conclusion, Mössbauer and NMR spectroscopies identify more than two distinct octahedral Fe ions that cannot be associated with two different integral valence states (2+, 3+), as the Verwey charge ordering model imposes.

3.2.2. Electronic spectroscopies. Several spectroscopies that allow study of the electronic structure in solid state physics have been applied to analyse the electronic state in magnetite. In spite of the extensive experimental work performed on this material, as we will show, no study was able to demonstrate the existence of two different octahedral iron ions in terms of valence states below the Verwey temperature. Moreover, some investigations show the lack of adequacy of the ionic CO model for the experimental observation. We would like to emphasize again that most of the studies use as a hypothesis this ionic model, i.e., the existence of octahedral Fe^{3+}, octahedral Fe^{2+} and tetrahedral Fe^{3+}, to explain the experimental spectra. In some cases, they are successful in reproducing a particular experimental spectrum, but the resulting physical parameters are obtained by fitting and not from independent models. In other cases, a model that seems valid for Fe_3O_4 cannot be extended to related compounds such as the substituted spinel ferrites. Finally, some recent experiments show the absence of charge ordering.

Core-level spectroscopies can, in principle, solve the problem of iron localization in Fe_3O_4. In fact, the binding energy of core-level electrons depends on their chemical state through the chemical shift. However, the different studies give contradictory results. Fe(2p) and Fe(3p) photoelectron spectra of pure Fe_3O_4 have been described as indicating a mixed valence oxide. But, while the Fe^{2+}/Fe^{3+} intensity ratio of the resolved components from the Fe(3p) spectrum

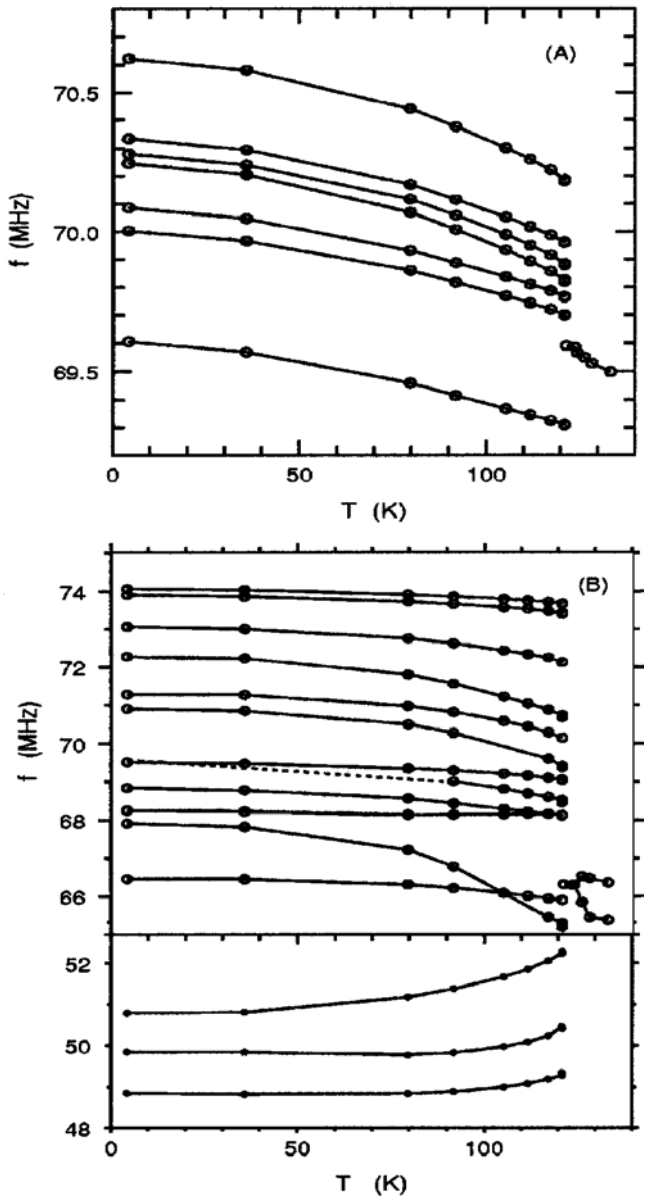

Figure 6. Temperature dependences of the NMR frequencies of lines corresponding to Fe ions on (A) tetrahedral and (B) octahedral sites. From [54].

agrees nicely with the stoichiometric value of 0.5, the Fe(2p) analysis of the spectrum gives a peak intensity ratio of 0.32, lower than the theoretical one [56]. Moreover, 3p–3d resonant photoemission shows that most of the resonant features in the Fe_3O_4 spectrum cannot be separated into contributions coming from either Fe^{2+} or Fe^{3+} [57].

Electron energy loss and x-ray absorption spectroscopies (XAS) are two other techniques very sensitive to the local structural and electronic state. Fe $L_{2,3}$ edges mark the electronic transitions from the 2p state to the projected local density of states of d character. So the

spectrum of Fe_3O_4 should be given by the addition of the three spectra corresponding to the three supposed different iron ions (A Fe^{3+}, B Fe^{2+} and B Fe^{3+}). The experimental L_3/L_2 spectra are very similar for different iron oxides [58–61]. Thus, the deconvolution into the respective individual components is highly dependent on the model and even the simulated theoretical spectrum qualitatively agrees with the experimental one. In addition, the theoretical spectrum is generally obtained by fitting the experimental one [59]. In other words, the parameters obtained from the analysis could only be considered physically relevant under the condition that the ionic model is valid. One point to emphasize here is that, for example, the proposed chemical shift between the two different octahedral sites (Fe^{2+}, Fe^{3+}) ranges from 0.7 [59] to 1.3 eV [61] showing the very low sensitivity of $L_{2,3}$ edges to the electronic state of the iron atom in these oxides. Recently, high energy resolution $L_{2,3}$ spectra of substituted spinels ($NiFe_2O_4$, $CoFe_2O_4$, Fe_3O_4, $MnFe_2O_4$ and $CrFe_2O_4$) have been measured [62]. The overall L_3 XAS profiles are very similar for the measured spinels pointing to a near independence of the spectra of the nominal valence state of Fe and/or the crystallographic site (see figure 7). We underline that $MnFe_2O_4$ and Fe_3O_4 L_3 spectra are nearly identical. We remember that manganese substitutes mainly at the tetrahedral site of the spinel structure and its formal valence state is 2+, there being Fe^{3+} instead of $Fe^{2.5+}$ in pure Fe_3O_4. The near identity of spectra for the different substituted spinels indicates that the local density of the empty d states seems to depend mainly on the crystallographic structure instead of on the local symmetry and the formal valence state. In this sense, the assignment of ionic d states in magnetite seems to lose its meaning showing that a large mixing of the iron states occurs, leading to the formation of a d band.

Similar points could be made for the L_3/L_2 x-ray circular magnetic dichroism (XCMD). The circular magnetic dichroic signal of Fe_3O_4 was measured by Kuiper *et al* [63] who interpreted the spectrum on the basis of the ionic model. They associated the three observed features with A Fe^{3+}, B Fe^{2+} and B Fe^{3+} signals as indicated in figure 8. We note here that in this interpretation they include a non-justified parameter to fit the spectrum. However, these three features cannot be assigned to the three valence states by comparison with related compounds. The XCMD spectra of highly iron defective magnetite including γ-Fe_2O_3, in which Fe^{2+} does not exist, show the same three-peak structure as is illustrated in figure 8. Moreover, the same three features were observed for substituted spinels where again they could not be assigned either to the local symmetry or to the valence state [64]. An interesting study was recently published in which the authors try to explain the electronic structure of magnetite below the Verwey transition by using the so-called local density approximation, LSDA + U, where a stable solution for the charge ordering state is obtained [65]. Within this description, they calculate the x-ray absorption spectra as well as the x-ray circular magnetic dichroism spectra at the K, $L_{2,3}$ and $M_{2,3}$ edges for several TM substituted Fe_3O_4 samples. In spite of the good agreement between theory and available experimental data, the study cannot be considered as a proof of charge ordering or localization. We would like to note that the two theoretical XCMD spectra, the Fe $L_{2,3}$ spectrum of $NiFe_2O_4$ and the Fe K spectrum of Fe_3O_4, do not reproduce the experiments at all (the reader can compare theoretical simulations given in [65] with experimental spectra given in [57] and [66]). Moreover, the ordering model used is the classical Verwey model that has been abandoned now. In addition, this model predicts a different magnetic moment for the iron B sites in Fe_3O_4—that is, goes against the experimental results where no differences in the magnetic moment have been observed. As a conclusion, an unrealistic model is able to fit reasonably some XCMD spectra but this fact leads one to discard it as a good model for supporting ionic localization in magnetite.

Oxygen K edge spectra of transition metal oxides were first reported by de Groot *et al* [67]. They analysed the spectra as divided into two regions: the first is a double peak, which can be

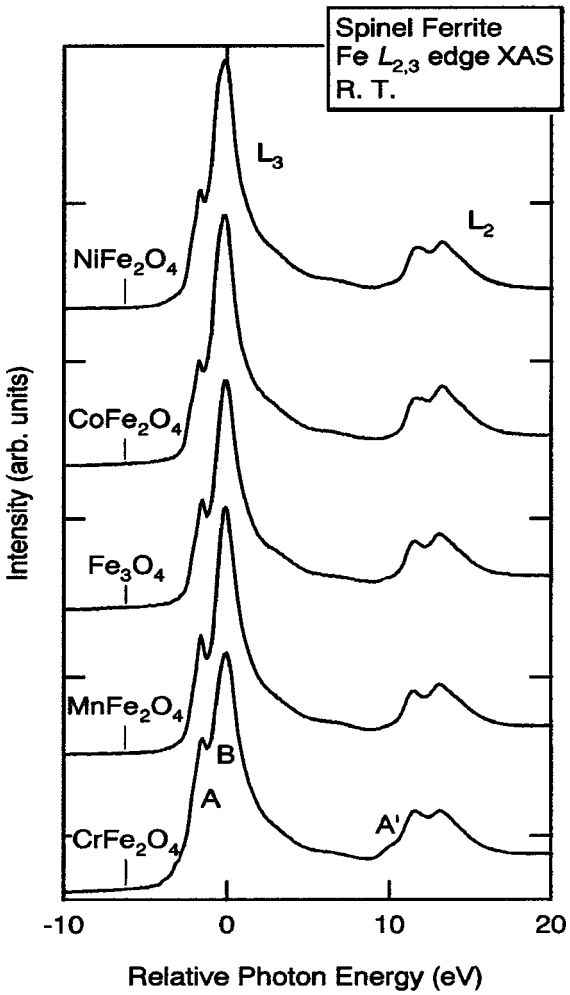

Figure 7. Comparison of Fe $L_{2,3}$ XANES spectra of several spinel MFe_2O_4 (M = Cr, Mn, Fe, Co and Ni) samples at room temperature with an applied magnetic field of 0.4 T. The zero in the energy scale is set at the Fe L_3 main peak. From [62].

related to the metal 3d states, and the second is a broader structure above the edge related to the 4s and 4p bands. The oxygen K edge spectrum is due to transitions from the 1s oxygen core state to the oxygen p projected unoccupied density of states. Thus, the assignment of the physical features, despite the wide consensus among the scientific community, to transition metal states with 3d character is at least risky. We do not enter into discussion of the different theoretical interpretations of the O K edge spectra, sometimes giving discrepancies between the results of different sets of authors and different electronic spectroscopies [67–70]. We want to analyse from the experimental point of view whether there are some physical features that allow the distinguishing of different valence states. First, O K edge XANES spectra of Fe_3O_4 and α-Fe_2O_3 are very similar to each other [67, 68, 70] even if the local symmetry and formal valence state for the Fe ion are different for each sample. Second, none of the authors try to reproduce the experimental spectra as sums of different contributions coming from different kinds of Fe ions in terms of symmetry and filling of the ionic d states. We would

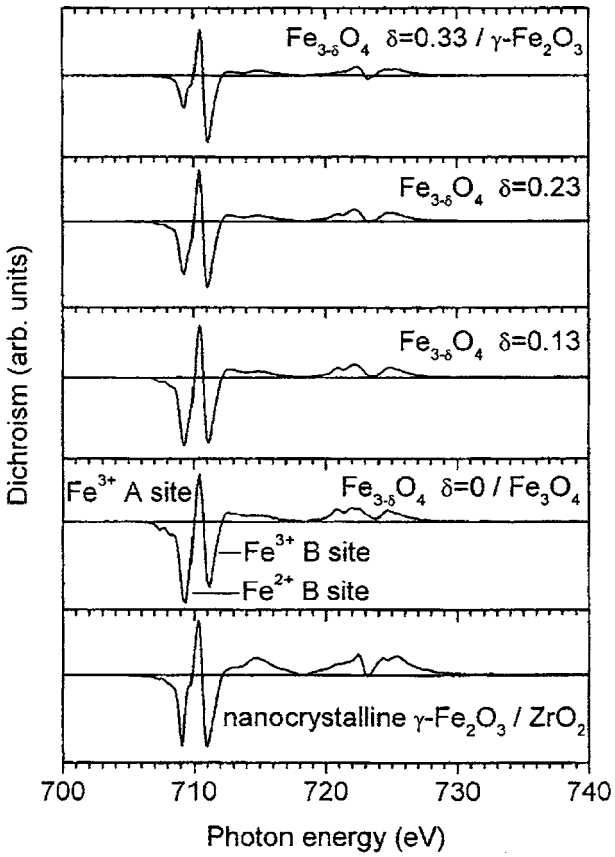

Figure 8. Fe $L_{2,3}$ XMCD spectra of non-stoichiometric $Fe_{3-\delta}O_4$ thin films compared to nanocrystalline γ-Fe_2O_3/ZrO_2. From [64].

also like to comment here on the interpretation given by multiple-scattering theory [70] for the O K edge spectrum of Fe_3O_4 without considering any kind of charge ordering. One needs at least a cluster of 69 atoms to reproduce the experimental spectrum. This means that the naive assignment of the pre-peak structure of O K edge spectra to ionic d states (t_{2g}, e_g) is far from reality when we need to include atomic shells beyond the first one in order to reproduce this feature well.

The valence photoemission spectra (PES) have also been the subject of many experimental studies [57, 71–75]. Photoemission spectroscopy (PES) and inverse photoemission spectroscopy (IPES) probe the density of occupied and unoccupied electronic states, respectively. In particular, valence photoemission gives information about the states close to the Fermi level. Because of the large overlap of Fe 3d and O 2p states in transition metal oxides, it is nearly impossible to detect the presence of two different ionic states by this technique. However, we can elucidate whether an excitation energy is required to create unbound holes and electrons entering the conductivity or whether there is a Fermi edge as in a metal. Recent PES studies have reported a reduction of the band gap, induced by the structural transition on heating through T_V, as the origin for the phase transition [74] instead of a complete collapse of this gap in the high temperature phase, first suggested by Chainani [71]. Moreover, an opening of a gap has also been detected by measuring the optical conductivity [73]. In addition,

band dispersions derived experimentally from PES agree reasonably well with band structure calculations for the high temperature phase [57]. Recent results from spin and angle resolved photoemission spectroscopy also provide a direct proof that the itinerant nature of the 3d electrons persists even at $T < T_V$ [75], showing that the Verwey transition affects mostly only the B site minority spin t_{2g} electrons.

In conclusion, most of the interpretation of the electronic and soft x-ray absorption spectroscopic data of Fe_3O_4 has been carried out from a localized electron point of view. However, recent experiments are demonstrating the inadequacy of the localized model for explaining the spectroscopic data.

3.3. Diffraction techniques

The technique able to determine a periodic ordering of physical entities is diffraction. X-ray and neutron diffraction techniques are the most powerful tools for determining the crystallographic structure. They have been mainly responsible for the microscopic knowledge of matter. However, the experimental verification of charge ordering by means of diffraction is a complicated problem, as we outline below. The difference in x-ray scattering power from atoms with different valence states is too small and consequently superstructure peaks coming from orderings of ions are very difficult to detect. The scattering power of x-ray diffraction depends on the total number of electrons on the atom, so the ability to discern one electron, the difference between Fe^{3+} and Fe^{2+} ions in Fe_3O_4, is very limited. Normally, crystallographic refinement uses the same scattering factors for different ionic states. The use of neutron diffraction does not resolve the problem although it can determine the magnetic structure in magnetically ordered systems and, hence, the value of the individual magnetic moments. However, if we do not consider the magnetic scattering, the interaction of neutrons with matter is nuclear and obviously is not sensitive to the electronic charge. So conventional diffraction is unable to detect in a direct way differences of electronic charge densities in a solid. Despite this, charge ordering can be inferred by means of diffraction in an indirect way, from the first-shell interatomic distances and from the magnetic moment localized on each atom. Recently, the use of x-ray synchrotron sources has allowed the development of a new technique, x-ray resonant scattering, which is able to detect a charge periodicity in a direct way.

3.3.1. X-ray and neutron diffraction results. How can diffraction data be used to differentiate between two kinds of metal ions (Fe in our case)? There are two main basic properties that can identify two kinds of Fe ions; the first one is the Fe–O interatomic distance and the second one is the local magnetic moment. Table 1 lists the interatomic Fe–O distances and magnetic moments for Fe^{2+} and Fe^{3+} ions in an octahedral and tetrahedral environment compared to the experimental values obtained for octahedral and tetrahedral iron atoms in magnetite below T_V.

(1) The appearance of distinct crystallographic sites for the metal ion has been considered as structural evidence of CO. However, the assignment to different valence states for the two ions in these different sites needs the extra condition that the metal–anion interatomic distance is near to the value corresponding to the associated valence state. For octahedrally coordinated iron oxides, the average interatomic distance for the cluster FeO_6^{3+} is about 2.025 Å, clearly distinguishable from that of the oxygen octahedron for the FeO_6^{2+} cluster, $d_{Fe-O} = 2.16$ Å [76]. Thus, a bimodal distribution of Fe–O interatomic distances must be found at the B site in Fe_3O_4 below T_V. Recent diffraction studies in magnetite by means of high energy transmission electron diffraction [77] have

Table 1. Fe–O bond distances and localized magnetic moment values for Fe ions in Fe_3O_4 compared to tabulated values for Fe^{2+} and Fe^{3+} ions given by Shannon *et al* [76].

High spin Fe ion	Average interatomic distance Fe–O (Å)	Localized magnetic moment (spin contribution) (μ_B)
$Fe^{2+}O_6$	2.16 ± 0.017	4
$Fe^{3+}O_6$	2.025 ± 0.017	5
$Fe^{3+}O_4$	1.87 ± 0.017	5
Octahedral $Fe^{2.5+}$ (Fe_3O_4)	2.058 ± 0.033[a] [78–80] 2.060[b] [26]	3.97 [20]
Tetrahedral Fe^{3+} (Fe_3O_4)	1.89 ± 0.01[a] [78–80] 1.884[b] [26]	3.82 [20]

[a] Structural determination by means of high resolution neutron and synchrotron x-ray powder diffraction.
[b] Structural determination by means of single-crystal neutron diffraction.

confirmed the neutron single-crystal structural determination of Iizumi *et al* [26, 78] at low temperatures. It is characterized by a fourfold monoclinic cell, $2\sqrt{a} \times 2\sqrt{a} \times 2a$, with Cc symmetry [26, 78, 79] compared to the cubic $Fd\bar{3}m$ high temperature structure. In all the studies, as was first pointed out by Iizumi, the Fe–O interatomic distances are intermediate between these corresponding to Fe^{2+} and/or Fe^{3+} ions, indicating that both powder and single-crystal diffraction are incompatible with the existence of Fe^{3+} and Fe^{2+} octahedra [80–82]. Moreover, all these studies agree that there are 16 different crystallographic sites for the octahedral Fe ion in the low temperature phase. Wright *et al* [80, 81] try to artificially split the four octahedra of their $P2/c$ refinement into pairs, with the aim of demonstrating the occurrence of charge ordering in magnetite, although their data in fact demonstrate the absence of such charge ordering [82].

(2) For magnetic atoms, another difference is in their local magnetic moment. Fe^{2+} and Fe^{3+} are both magnetic ions with a distinct local magnetic moment. It is obvious that if an ion is called Fe^{2+}, its magnetic moment should be near to the theoretical value of 4 μ_B. Moreover, two different magnetic moments should be easily detected if two Fe ions are present in the sample by means of neutron scattering, as the neutron scattering factor depends on the local magnetic moment. Actually, this is the standard technique for determining local magnetic moments and their ordering in magnetically ordered systems. The determination of the magnetic moments merits an extra discussion. The measured magnetization (-4 μ_B) agrees well with a model of localized electrons: in the Néel model of ferromagnetism the tetrahedral A sublattice is antiferromagnetically coupled to the octahedral B one, so the total magnetization observed was $M = \mu(\text{octahedral } Fe^{3+}) + \mu(\text{octahedral } Fe^{2+}) - \mu(\text{tetrahedral } Fe^{3+})$. The magnetic contributions of trivalent tetrahedral and octahedral $Fe^{3+}(d^5)$ ions are mutually compensated so only magnetic moments of octahedral $Fe^{2+}(d^4)$ ions are contributing to the macroscopic magnetization, which corresponds closely to the high spin octahedral Fe^{2+} contribution of 4 μ_B. This fact, in our opinion a coincidence, was taken as a proof of the existence of atomic electron localization. Polarized neutron diffraction experiments have shown that the magnetic moment of the Fe ion at the A site is 3.82 μ_B, instead of 5 μ_B [20]. Moreover, low temperature neutron diffraction experiments were not able to detect any difference between magnetic moments of Fe ions on the B sites [3, 26, 81]. No new magnetic reflection associated with the ordering of octahedral B irons (Fe^{3+}, Fe^{2+}) has been observed. In addition, the magnetic moment measured on the B sites is 3.97 μ_B [81],

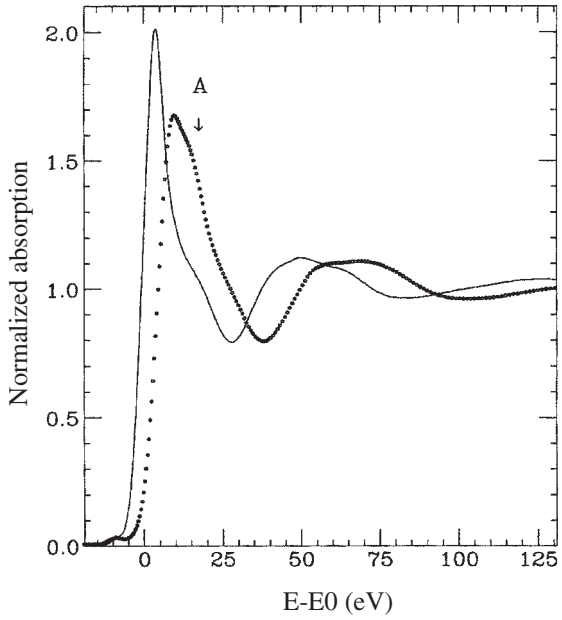

Figure 9. Normalized XANES spectra of Fe^{2+} (solid curve) and Fe^{3+} (dots) water complexes with pH = 1 on a relative energy scale. About 4 eV separates the absorption edges. From [83].

a value very similar to that for the tetrahedral A site, which implies that the assignment of the tetrahedral Fe ion to a 3+ valence state is also not well supported experimentally.

3.3.2. X-ray resonant scattering. We will continue the discussion of the applicability of x-ray resonant scattering for the determination of different valence states in a solid. As we have outlined before, x-ray resonant scattering deals with the study of very weak or forbidden reflections. In this case, the observed resonance (a sharp increase of the scattered intensity at the absorption edge) marks the difference between the anomalous atomic scattering factors of a selected atom in the lattice. Because the atomic scattering factors (or the x-ray absorption coefficients) are different for atoms with different valence states, this technique is suitable for determining the occurrence or absence of ionic charge ordering in mixed valence compounds such as Fe_3O_4. However, the experimental results have been heavily criticized in a recent topical review by Walz [7]. In the following, we will explicitly refute all these unsupported criticisms, showing the great potential of this relatively new technique for the determination of electronic information on solid state materials.

It is well known that x-ray absorption spectroscopy is able to distinguish different ionic valence states through a chemical shift of several electronvolts in the XANES spectra. Figure 9 shows a comparison of octahedral water complexes of Fe^{3+} and Fe^{2+}, showing the energy shift (chemical shift) of the absorption edge [83]. Intimately correlated with the XANES spectra is the anomalous part of the x-ray atomic scattering factor, $f(E) = f'(E) + \mathrm{i}f''(E)$. The energy dependence of the imaginary part of the scattering factor, f'', is proportional to the x-ray absorption coefficient $\mu(E)$ through the optical theorem and the real part, $f'(E)$, is causally related to $f''(E)$ by the Kramers–Kronig transformation [84]. We note that at energies close to the absorption edge, a remarkable contrast between the atomic scattering factors of octahedral

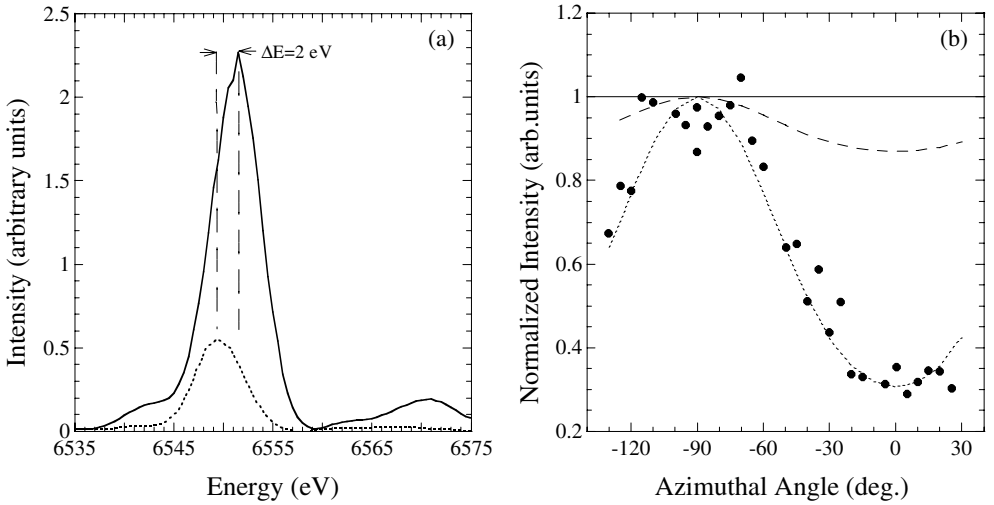

Figure 10. (a) Calculated intensity terms $[f_{Mn^{4+}} - f_{Mn^{3+}}]^2$ (solid curve) and $[f^{par}_{Mn^{3+}} - f^{perp}_{Mn^{3+}}]^2$ (dashed curve) corresponding to CO (charge ordering) and ATS (so-called orbital ordering) reflections, respectively. Note that the CO reflection has been calculated in terms of the chemical shift between the experimental reference XANES spectra for Mn^{3+} and Mn^{4+} ions and the ATS reflection considering the anisotropic splitting due to the Jahn–Teller distortion of the Mn^{3+} ion [85]. (b) Azimuthal behaviour of the $(0k0)$ CO reflection of $Pr_{0.6}Ca_{0.4}MnO_3$ reported in [89] (full circles) compared with different theoretical models: (i) the pure charge ordering model (solid curve), (ii) a realistic charge ordering model including an anisotropic splitting of 2 eV (dashed curve) and (iii) a structural model [85] including a Thompson term $C = 0.5$ (dotted curve).

Fe^{3+} and Fe^{2+} is obtained, which makes it possible to discriminate between the two electronic states. In fact, the anomalous scattering amplitudes of Fe^{3+} and Fe^{2+} in crystallographically equivalent octahedral sites are not the same and non-zero resonant scattering intensity coming exclusively from the difference of charge density should be observed.

On scanning these forbidden reflections (forbidden by glide-plane and/or screw-axis selection rules) as a function of the photon energy across the transition metal (Fe) absorption K edge, an intense resonance at the threshold energy should be observed. Figure 10(a) shows a typical resonance for a pure charge ordered Mn^{3+}–Mn^{4+} reflection (from [85]). This method has also been extensively used to demonstrate the existence of charge ordering in manganites but, as we will show, there is no ionic ordering in that case either.

As we commented before, a strong resonance can also be observed, due to ATS reflections. In fact, the anomalous scattering factor (i.e. the x-ray absorption coefficient) is anisotropic when the resonating atoms are in an anisotropic crystalline environment [86]. For dipolar electronic transitions (the main contribution) the atomic anomalous scattering factor will no longer be a scalar but will now be a two-range tensor giving rise to the appearance of resonant reflections produced by the presence of anisotropy of the tensor of x-ray susceptibility (called ATS reflections) [87, 88]. This anisotropy of the x-ray susceptibility has a significant value in resonant conditions (at the absorption edge). One of the characteristics that differentiates a charge ordering (CO) reflection from an ATS reflection comes from the intensity of the resonance, as illustrated in figure 10(a), but the most important difference is in its azimuthal behaviour; figure 10(b) shows the azimuthal evolution of the resonance intensity for a CO reflection, a combined charge and anisotropic reflection and a pure anisotropic reflection. It

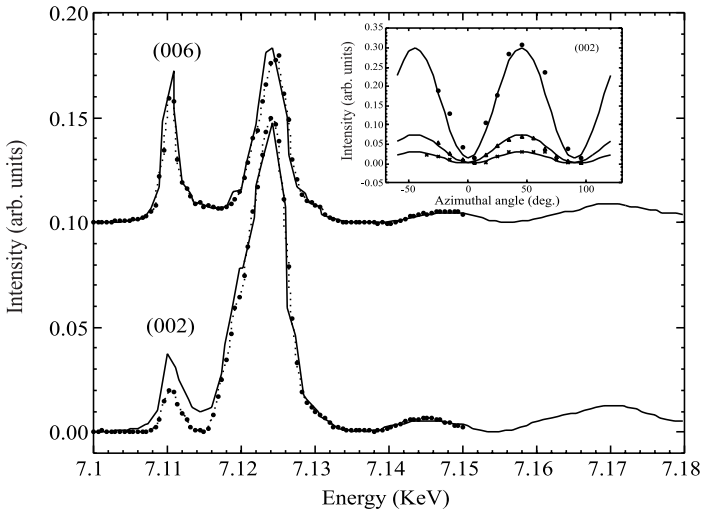

Figure 11. Integrated intensity of $(0\,0\,4n+2)$ forbidden reflections versus photon energy in magnetite as a function of temperature; $T = 300$ K (solid curve) and $T = 30$ K (full dots). Inset: the azimuthal dependence for the (002) reflection at 30 K and fixed energies: 7124.5 eV (Fe K edge; circles), 7111 eV (pre-peak; triangles) and 7135 eV (EXAFS region; crosses). From [14, 15].

can be observed that no charge order is deduced for the $Pr_{0.6}Ca_{0.4}MnO_3$ sample [89]. In this case, the scattered intensity depends on the relative orientation of the x-ray polarization vector with respect to the local anisotropy axis. For dipolar–quadrupolar transitions and pure quadrupolar transitions the scattered intensity also depends on the momentum transfer [90–92]. These ATS reflections have been considered by some authors as a proof of d orbital ordering due to their azimuthal periodicity; i.e. their intensity may vary during crystal rotation around the diffraction vector. This azimuthal dependence is the main criterion for differentiating between reflections coming from charge ordering and from anisotropy of the charge density. No azimuthal dependence should be observed for a pure charge ordering reflection.

X-ray resonant experiments at the Fe K absorption edge of the (002) and (006) forbidden reflections have recently been published [14, 15, 93, 94]. We refer the reader to these publications for details. We will summarize the main results here. At room temperature the resonant spectrum shows the absence of scattering intensity at energies below the Fe K edge, as expected for pure forbidden reflections. Scattered intensity is only observed at energies above the absorption edge, showing that the reflection arises from the anomalous part of the iron atomic scattering factor. The energy and azimuthal dependences for both forbidden reflections are shown in figure 11. Three main features can be distinguished in the energy dependence, and these are described as follows: the resonance at the energy of the pre-peak of the fluorescence spectrum coming from dipolar–quadrupolar transitions at the iron tetrahedral sites; the main resonance, at the absorption edge, coming from dipolar transitions at the pseudo-octahedral iron ions; and the oscillatory behaviour above the absorption edge (corresponding to the EXAFS region). We will deal here only with the main resonance due to the octahedral ions. The real site symmetry of the B atoms is trigonal ($\bar{3}m$) so the dipolar atomic scattering factor is anisotropic with two degenerate components, along the direction of the trigonal axis and its perpendicular. The appearance of this resonance arises from the different orientation of the trigonal axis in the octant of the unit cell. In other words, the

anomalous scattering tensor for $(0\,0\,4n+2)$ reflections is given by

$$F = \begin{pmatrix} 0 & f_{xy} & 0 \\ f_{xy} & 0 & 0 \\ 0 & 0 & 0 \end{pmatrix}$$

where $f_{xy} = (16/3)(f_{\parallel} - f_{\perp})$, $f_{\parallel}$ and $f_{\perp}$ being the components of the atomic scattering tensor parallel and perpendicular to the trigonal axis of each of the pseudo-octahedral Fe B ions. The energy and azimuthal dependences are well explained by just taking into account the anisotropy of the atomic anomalous scattering factor of these Fe B atoms, being identical for the different B sites in an octant. It is worth noting that the energy dependent spectra taken at different azimuthal angles can be superimposed if we multiply each of them by the azimuthal dependence. Taking into account that there are four octants in the high temperature unit cell, this means that the average anomalous atomic scattering factor taken for four octahedral ions with the same trigonal axis orientation is the same as the average for the Fe(B) ions in the other three possible trigonal orientations. There are different possibilities for giving a coherent explanation for these high temperature data:

(I) All the iron ions are electronically equal. This is the more natural explanation and it coincides with the structural determination where only one crystallographic position for the octahedral atom is obtained.

(II) If the anomalous scattering factor depends on the valence states of different Fe^{3+}–Fe^{2+} atoms, the charge must fluctuate on a timescale faster than 10^{-16} s (the interaction time for the photoabsorption process) and the incident photon would see a random distribution of different atomic scattering factors of the Fe^{3+} and Fe^{2+} states. Accordingly, no coherence requirement for diffraction would be fulfilled.

(III) We can hypothesize that the difference between Fe^{3+} and Fe^{2+} scattering factors is mainly due to the chemical shift, the anisotropy splittings being similar for Fe^{3+} and Fe^{2+} for both ions. In that case, the shape of the main resonance as a function of energy must show a double peak instead of a single peak as observed experimentally.

If we consider the charge segregation to be proportional to the chemical shift, the maximum charge disproportionation should be approximately 0.25 e^-. As a conclusion of this analysis we can say that the mobile electron is not localized at the octahedral iron atom, at least for timescales above 10^{-16} s. In other words, the electrical conductivity must be explained in terms of a band transport model.

We have also performed the same experiments below the Verwey transition temperature without and with an applied magnetic field in order to orient the low temperature crystallographic *c*-axis. The energy and azimuthal dependences of the (002) and (006) forbidden reflections were the same as for room temperature data (see figure 11). The absence of any changes between the experimental spectra above and below T_V and between non-oriented and partially oriented samples shows that the same conclusions as obtained for the high temperature phase can be applied to the low temperature phase, i.e. any charge disproportionation should be less than 0.25 e^-. Moreover, the experiment at low temperatures demonstrates that non-integral charge ordering, with $(0\,0\,4n+2)$ periodicity, should be present. In other words, the difference in average charge between consecutive octahedral iron planes should be zero for all of the three crystallographic directions of the low temperature phase. From this argument, we can conclude: first, eight of the models for the low temperature monoclinic *Cc* structure proposed by Zuo *et al* [15, 77] are incompatible with this x-ray resonant scattering experiment; second, the charge segregation in the low temperature phase, if it exists, should be less than 0.25 e^-; and third, if some charge disproportion exists, the ordering

scheme cannot satisfy Anderson's condition. Assuming that no ionic charge ordering exists in magnetite, we can consider that the low temperature phase is characterized by the existence of more than two different octahedral ions, as the crystallographic determination [26, 81] and the recent NMR analysis imply [54, 55]. Recent x-ray anomalous scattering experiments have been performed on (0, 4, 1/2)-type superlattice and (003) reflections at $T < T_V$ [95, 96]. However, more detailed study of their energy, azimuth and polarization dependences is needed in order to obtain information related to the charge disproportionation in the low temperature phase of magnetite.

As a last point of discussion, we would like to comment on the results of Sasaki *et al* [97] and Toyoda *et al* [96]. They have been claimed by Walz as direct evidence of the existence of an Anderson short range order (SRO) by using the valence difference contrast method (VDC) for a range of temperatures across T_V. Sasaki *et al* reported a chemical shift between the structure factors of the A (T_d) and B (O_h) sites $\delta E = 2.5$ eV that corresponds to a valence difference of 0.5 e^-, intermediate between those of Fe^{3+} and Fe^{2+} estimated for the octahedral iron atoms from XANES spectra [97]. This valence difference does not imply the existence of Fe^{3+} and Fe^{2+} iron species at the octahedral sites. In fact, the same intermediate chemical shift should be observed for an intermediate valence state $Fe^{2.5+}$ for the octahedral iron atoms. We refer the reader to a similar case in the so-called charge ordered manganites; an intermediate chemical shift is obtained for $Mn^{3.5+}$ samples but the absorption spectrum cannot be deconvoluted as a sum of those for two Mn ions with two different 3+ and 4+ valence states [98, 99]. Figure 12 illustrates this fact. On the other hand, Toyoda *et al* found a chemical shift of approximately 1 eV between A and B sites. As the ideal chemical shift would be 2.5 eV between $Fe^{2.5+}$ in the B sites and Fe^{3+} in the A sites, the valence difference corresponds to 0.2 e^- [96]. Thus, in the case of magnetite, it is not possible to carry out this VDC analysis as we have no means of discerning whether the average spectrum is the sum of two components (octahedral and tetrahedral irons) or three components (octahedral Fe^{2+}, octahedral Fe^{3+} and tetrahedral Fe^{3+}), according to the ionic model. Thus, the use of the VDC method to show directly the occurrence of Fe^{3+}–Fe^{2+} charge ordering is inappropriate.

4. Verwey-type compounds

The order–disorder model proposed by Verwey for magnetite has been the basis for the so-called Verwey-type phase transitions in related transition metal oxides. Moreover, electronic conduction in oxides has been interpreted in terms of atomic localization of the electronic states [1–8, 100]. In this section, we will deal with some mixed valence oxides, which undergo metal–insulator phase transitions that have been classified as of charge ordering type. We will show that a complete analogy to magnetite cannot be made for these compounds, but there are no experimental proofs demonstrating the expected ionic ordering in these so-called Verwey-type compounds either.

The first oxide group comprises the RFe_2O_4 (R = rare earth) compounds which are known as iron mixed valence systems. In these compounds, as in Fe_3O_4, the formal valence of the iron ion is 2.5 and no atomic disorder is found in the high temperature phase. The most studied sample of this family is YFe_2O_4. This compound shows a two-step Verwey-type metal–insulator phase transition at about 240 and 200 K [101–104]. These first-order phase transitions are also accompanied by the distortion of the hexagonal lattice at RT to a monoclinic and subsequently to a triclinic one. However, as was pointed out by Brabers [5], the electrical conduction in these rare earth compounds is quite different from that in magnetite. The electrical resistivity shows a large anisotropy; it is two orders of magnitude along the *c*-axis lower than in the *ab* plane and the value of the room temperature resistivity is about

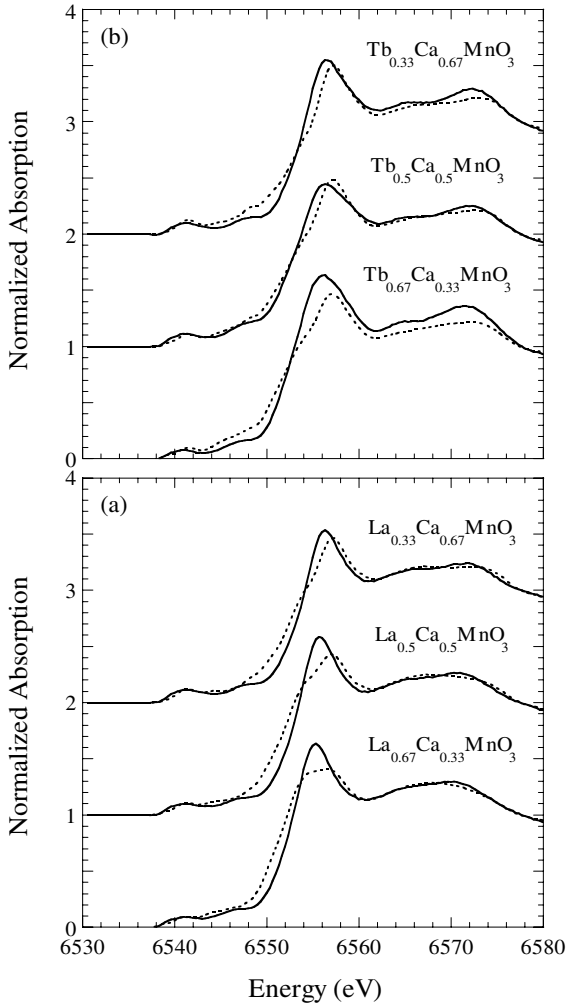

Figure 12. Comparison between experimental high resolution XANES spectra at the Mn K edge of the (a) $La_{1-x}Ca_xMnO_3$ and (b) $Tb_{1-x}Ca_xMnO_3$ series (solid curve) and simulations obtained by weighted linear combination of the spectra of the respective end-member compounds (dashed curve). From [99].

10^2 Ω cm, comparable to the room temperature value of the resistivity in magnetite [104]. Furthermore, another notable difference is in the magnitude of the pressure effect on the Verwey transition [105]. In addition, the magnetic coupling between iron ions is antiferromagnetic for the RFe_2O_4 compounds in contrast to the ferromagnetic coupling between octahedral iron ions in magnetite. There remain only two analogies with magnetite: first, the structural phase transition is accompanied by a sharp discontinuity in the resistivity; and second, the Verwey transition in RFe_2O_4 is also strongly affected by the oxygen stoichiometry (1% of oxygen deficiency is enough for complete disappearance of the transition) [105].

Like for magnetite, the low temperature charge ordering scheme has not been determined yet. Nagakawa *et al* [102] determine two crystallographic phases corresponding to the two-step transition in YFe_2O_4 whereas Iida *et al* [103] indexed the low temperature diffraction pattern

assuming a monoclinic phase in $ErFe_2O_4$. Neither of the two determinations gives a detailed description of the crystallographic structure but it is expected that for a triclinic structure as proposed for YFe_2O_4 more than two inequivalent crystallographic sites exist for iron atoms. Recently, x-ray and neutron diffraction studies have been performed on $LuFe_2O_4$ [106] and they showed the following sequence of structural phase transitions: disorder–2D CDW (charge density wave)–3D CDW. The ground state of the low temperature phase is characterized by an incommensurate charge density wave state. In their interpretation, the authors conclude that the 3D CDW state is not the fully ordered ground state but still contains considerable randomness. In other words, the low temperature phase is not a charge ordered state as was initially postulated. A similar conclusion can be deduced for the YFe_2O_4 system; Ikeda *et al* [107] show that at low temperatures five different phases coexist without defining the charge ordering of these phases. As we have said for magnetite, no experimental proof of ionic charge ordering in these RFe_2O_4 compounds has been given yet.

A second group of mixed valence iron oxides where charge ordering has been proposed includes the double-cell perovskites $REBaMe_2O_5$ (RE = Y, Tb, Sm, Nd; Me = Fe, Co, Mn) [108–111]. In this case, two different crystallographic sites for the Fe ion are present in the ordered low temperature phase so the assignment of each of these crystallographic sites to two different valence states is clearer. All these compounds show a discontinuity of the electrical resistivity at the structural phase transition. Simultaneously with the structural transition, a magnetic ordering occurs, so the two iron atoms must show different magnetic moments too. Generally, two parameters have been used to assign each of the crystallographic sites to an integral valence state. The first one is the interatomic Fe–O distance, obtained by applying the bond valence sums (BVS) method, which is a very good method for empirically determining the valence state. Second, the localized magnetic moment should correspond to the theoretical (or experimental) one corresponding to the different iron valence state. In table 2, bond valence sums and magnetic moments are given for different so-called charge ordered materials, associated with the respective numbers of inequivalent crystallographic sites in the structure. In all the cases, the bond valence sums and the magnetic moments are different from those related to the integer valence. Thus the existence of two different crystallographic sites does not guarantee the existence of two integral valence states. In relation to this, we would like to emphasize that, on the other hand, a high degree of charge disproportionation exists and many authors refer to it with this clear definition.

The series $La_{1-x}Sr_xFeO_3$ [112] shows a phase transition from a high temperature paramagnetic state to a low temperature antiferromagnetic state where an apparent ordering of Fe^{3+} and Fe^{5+} ions has been proposed. However, all the Fe atoms have the same local environment over the whole temperature range and the observed magnetic moments at the nominal Fe^{3+} and Fe^{5+} sites support a model based on the existence of charge disproportionation, i.e. non-integral charge states, in this sample.

Mixed valence manganese oxides are another class of transition metal oxides that exhibit the so-called charge ordering phase transitions. The recent interest in the study of mixed valence manganites is due to the observation of colossal magnetoresistance in the series $RE_{1-x}Me_xMnO_3$ (RE = rare earth, Me = divalent metal). Several reviews have been published on the physics of these systems and we refer the reader to them for a general discussion [6, 113–115]. We will only deal here with the proposed charge ordering states for compositions where the manganese ion is in the 3.5+ formal valence state ($Nd_{1/2}Sr_{1/2}MnO_3$, $La_{1/2}Ca_{1/2}MnO_3$, $Pr_{1/2}Ca_{1/2}MnO_3$ and $La_{1.5}Sr_{0.5}MnO_4$). These materials undergo a structural phase transition as a function of temperature with a discontinuity in the electrical resistivity, the most insulating phase identified as being a charge ordering phase. The experimental reasons supporting this identification have initially come from neutron, x-ray diffraction and electronic

Table 2. Bond valence sums (BVS) and magnetic moments of several so-called charge ordering TM oxides, which undergo charge disproportionation (% CD).

Compound	Bond valence determination		CD	No ineq.	Magnetic moments		References
	$M^{n+\delta}$	$M^{n-\delta}$	(%)	sites	$M^{n+\delta}$	$M^{n-\delta}$	
Fe_3O_4	2.72	2.51	21	4[a]	4.17	4.17	[81]
$YBaFe_2O_5$	2.94	2.23	71	2	3.82	3.82	[109]
$YBaCo_2O_5$	2.69	2.02	67	2	4.2	2.7	[109, 110]
$TbBaFe_2O_5$	2.76	2.37	39	2	4.15	3.65	[111]
$Ca_2Fe_2O_6$	4.58	3.48	55	2	2.5	3.5	[140]
$La_{1-x}Sr_xFeO_3$	4.2	3.4	40[b]	1	2.72	3.61	[112]
$La_{0.5}Ca_{0.5}MnO_3$	3.88	3.42	46	3	2.57	2.98	[117]
$Nd_{0.5}Sr_{0.5}MnO_3$	3.98	3.49	49	2	2.8	3.0	[139]
$Pr_{0.5}Ca_{0.5}MnO_3$					2.75	3.18	[121]
$NdNiO_3$	3.23	2.78	45	2			[138]
$YNiO_3$ (Ho, Er, Tm, Yb, Lu)	3.24	2.58	56	2			[134]
α-NaV_2O_5	4.51	4.46	4[c]	6			[137]

[a] The four inequivalent sites B(1)–B(4) in the orthorhombic *Pmca* unit cell represent an averaging over 4 of the 16 inequivalent B sites in the larger *Cc* supercell.
[b] The charge disproportionation reported by Battle *et al* [112] has been calculated from Mössbauer experiments.
[c] Calculations performed using the FDMNES code [155] result in a CO of a small fraction of the electron (0.04 e^-) to fit the x-ray resonant scattering data [137].

microscopy. X-ray and neutron diffraction allow one to determine that the one-site Mn ion of the high temperature phase is transformed into three inequivalent crystallographic sites in the CO phase. Two of them are very similar in terms of distribution of Mn–O distances so the authors associate them with only two different atoms, i.e. Mn^{3+} and Mn^{4+} ions [116–118]. The identification of two different Mn ions was also performed by means of electron microscopy. In this case, the electronic image shows stripes with a periodic ordering that has also been described as due to the ordering of Mn^{3+} and Mn^{4+} ions [119, 120]. Figure 13 shows an electronic image of the La:Ca 1/2:1/2 sample. Needless to say, there are solid proofs of the existence of two different Mn ions in the charge ordering phase, but neither neutron diffraction nor electronic microscopy can confirm the identification of these as Mn^{3+} and Mn^{4+} ions. In fact, the bond valence sums method gives a value for the valence state of the formal Mn^{3+} ion that differs from that of Mn^{3+} in $LaMnO_3$. Moreover, the distribution of Mn–O distances also differs from the local tetragonal distortion of $LaMnO_3$ [117, 118, 121]. The same can be said for the assumed Mn^{4+} ion. In addition, the magnetic moments on each of the two sites are very similar to each other and disagree with the expected magnetic moment for pure ionic Mn^{3+} or Mn^{4+} [122].

In order to demonstrate the existence of real charge and orbital ordering, x-ray resonant scattering experiments have been performed on these materials [123–127]. In spite of the very good experimental data, the interpretation of these x-ray resonant scattering experiments has been performed in a very naive and non-rigorous way. Most of the papers claim the existence of ionic charge and d orbital ordering in these systems and some reviews refer to them as experimental demonstrations of charge and orbital ordering. A detailed analysis of the x-ray resonant scattering data and their comparison with high resolution x-ray absorption spectra have shown that no real charge ordering occurs in manganites [85, 99]. Moreover, anisotropy-induced reflections cannot be considered as an experimental proof of d orbital

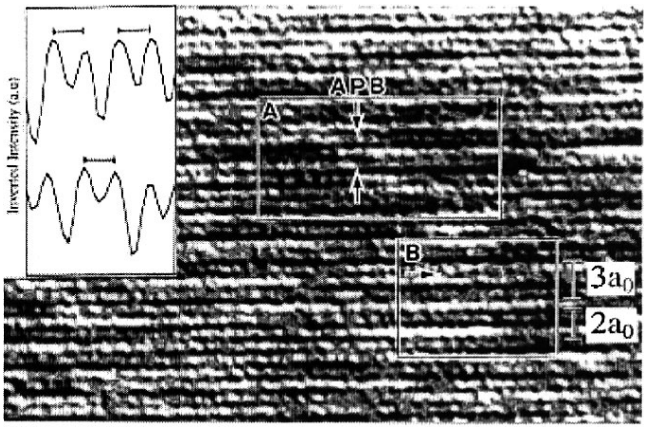

Figure 13. A high resolution lattice image of nearly commensurate charge ordering in $La_{0.5}Ca_{0.5}MnO_3$ at 95 K. Residual discommensurations are indicated by arrows in boxed area A whereas antiphase boundaries of paired Jahn–Teller stripes (JTS) are highlighted in boxed area B. The inset shows intensity profiles from two immediate regions of paired JTS separated by an antiphase boundary, showing a phase shift of π. From [120].

ordering [89, 128, 129]. Recently, some of the authors that claimed charge and orbital ordering are reconsidering their conclusions, admitting that no integer charge ordering occurs in these compounds [130, 131]. On the other hand, the so-called charge/orbital phase transition can be easily explained as a structural phase transition driven by a softening of a phonon mode, giving a new periodicity of the oxygen atoms [85]. The coupling of the electronic states with phonons would be the responsible for the change in the electrical properties of the system. We would like to emphasize that the so-called CO is characterized by the presence of two different types of Mn atom with different local geometrical structure in that case. This fact implies that the total charge on each atom should be different and the charge density should show spatial anisotropy induced by the local geometrical structure.

Finally, valence states such as Ti^{3+} and Ti^{4+} in Ti_4O_7 [132] and V^{4+} and V^{5+} in α-NaV_2O_5 [133] as well as charge disproportionation ($Ni^{3+\delta'}$ and $Ni^{3-\delta}$) in $NdNiO_3$ have recently been reported [134]. X-ray resonant scattering experiments have also been performed on these transition metal oxides, but no complete charge segregation has been observed experimentally (see table 2). α-NaV_2O_5 was studied by Nakao *et al* [135] and Grenier *et al* [136] who claim a charge segregation of about 0.5 e^-. A re-analysis of the data by Joly *et al* [137] obtained a charge segregation lower than 10%. $NdNiO_3$ was studied by Staub *et al* [138] and they obtained that the $Ni^{3+\delta'}$–$Ni^{3-\delta}$ charge segregation is about 0.5 e^- in the insulating low temperature phase.

5. Theoretical implications

The theoretical descriptions of metals, semiconductors, insulators and the transitions between them were initially based on a model of non-interacting or weakly interacting electron systems. Within the pure band theory [141, 142], the highest valence band is completely filled in the insulator state and for metals this upper band is partially filled. In other words, the Fermi level lies in a band gap for insulators while it is inside a band for metals. This basic distinction between metals and insulators in terms of filling of electronic bands was established in the early years of quantum mechanics [141–143]. Although this band picture was successful in many respects, de Boer and Verwey [144] reported that many transition metal oxides with

partially filled d electron bands were often insulators. As a typical example in their report, there is the case of NiO. Concerning this controversy, Mott [24, 145, 146] was the first to point out the relevance of electron–electron correlation as a possible origin for the insulating behaviour in many transition metal oxides. In this way, the field of study of strongly correlated electron systems was born with the goal of understanding how oxides with partially filled d bands could be insulators and how an insulator (the so-called Mott insulator) becomes a metal as some controllable parameters are varied. In theoretical approaches, Mott took the first important step towards understanding how electron–electron correlation could explain the insulating state.

The basic ingredients for the theory of transition metal oxides are nearly the same as those that de Boer and Verwey propose [144] in the so-called 'hopping conduction'. They envisaged NiO, CoO, MnO, Fe_2O_3, Fe_3O_4, Mn_2O_3, Mn_3O_4 and Co_3O_4 as being highly ionic, the oxygen ions all being O^{2-}, whereas the metallic ions are all nominally in 2+ or 3+ states. They recognized, by simply counting the number of 3d electrons, that this implies partially filled 3d bands and, according to the Bloch band picture, all these compounds should be metallic. They suggested that when the barrier to the tunnelling of 3d electrons between neighbouring cations is large, the system behaves as an insulator. Furthermore, they correlated the height of the barrier with the Coulomb repulsion between the 3d electrons. They also inferred that an integral number of d electrons per cation is necessary for the insulating configuration. Within this framework, the electrical conductivity behaviours of magnetite and the so-called Verwey transition were naturally explained as due to ionic ordering of the high temperature fluctuation of the electron between Fe^{2+} and Fe^{3+} ions. The consideration of the transition metal oxides as highly ionic systems has continued to this day, and may have originated from the supposed experimental confirmation of the Verwey ordering model of magnetite. At this point, we would like to emphasize that the Verwey ordering model was considered as experimentally proved from the 1950s nearly to the 1980s. Over this period of time, in which there was great activity in this field, this assumption determined the whole theoretical development.

The most widely accepted attempt to explain the breakdown of the pure band theory for explaining the conduction in TM oxides comes from the ideas of Mott. There is now a brief discussion of Mott's ideas; we consider hydrogen atoms in a one-dimensional array. This array will be a metal if the interatomic hydrogen distance is small and the probability of an electron transferring from one atom to a neighbour is large enough. Electrons should move so fast that the Coulomb interaction between them is averaged and the Hartree–Fock approximation for the potential is applicable. If we apply this approximation, the electron number is one per atom, and since one orbital state can contain two electrons with opposite spins, we have a half-filled band. Within this framework the system is a metal showing only Pauli paramagnetism. If we increase the interatomic distance gradually, the first effect is a decrease of the bandwidth correlated with an increase in the density of states. Mott argued that this description is insufficient because the Coulomb repulsion between electrons is ignored. Since the Coulomb interaction is determined by the distance between electrons, a phase transition from a metal to an insulator state occurs at some critical value of the bandwidth. In the limit of zero bandwidth or an array of far-distant atoms, the appropriate quantum description is in terms of atomic wavefunctions instead of extended Bloch waves. If one atom loses its electron, the energy of the excited state is higher than that of the ground state by the on-site Coulomb energy U. Since a finite energy is needed to excite the system, a weak external field cannot change the state of the system and no electrical current is induced. This situation will not change even for a finite transfer integral, if it is small compared with U. This problem was partially resolved by Hubbard by considering a model Hamiltonian where only the on-site Coulomb interaction U is taken into account [147–149]. However, this model implies some simplifications when it is applied to d electron TM systems.

It assumes that the orbital degeneracy of d orbitals is lifted by a crystal field; it does not consider the overlap between the d band and the p band of ligand atoms and it neglects the inter-site Coulomb force V. In spite of these simplifications, Mott's ideas and the Hubbard model have been very successful and they are the basis of the supposed present-day knowledge of transition metal oxides. The Mott classification of conductors and insulators has been recently expanded as a result of considering an aspect of the orbital degeneracy, as it is the overlap or the closeness of the d band and the p band of ligand atoms which bridges between the elements in transition metal compounds. For example, in TM oxides the oxygen $2p_\sigma$ level becomes close to that of the partially filled 3d band near the Fermi level. Thus the charge gap of the Mott insulator cannot be accounted for solely with d electrons, and p electron degrees of freedom should also be considered. In this case, if the p_σ level becomes closer to the d states, the character of the minimum charge excitation gap changes to that of a gap between a singly occupied d band with a fully occupied p band and a non-fully occupied d band with a p hole. This kind of insulator was proposed by Zaanen *et al* [150] as a charge-transfer (CT) insulator as contrasted with the Mott–Hubbard insulator (MH), in which the band gap formation is due to the splitting of the d band into lower and upper Hubbard bands, separated by the on-site Coulomb interaction.

As we have briefly argued, the main ingredients of the description of 3d transition metal oxides are the following:

(i) Generally, d electrons are mainly considered localized on the atoms, so the atomic d orbitals are used as basis functions to describe the solid. This is the basis of the tight-binding model, considered appropriate for describing TM oxides.
(ii) Due to the strong localization of the 3d electrons on the atom, the intra-atomic Coulomb repulsion (U) is assumed to be the relevant parameter as regards the electronic state of TM oxides.

Although these two premises seem generally accepted nowadays, we consider that there are still no solid reasons to consider them to be experimentally proved. The most often claimed experimental proof for electron localization is the value of the local magnetic moments determined by means of neutron diffraction. For instance, the agreement between the experimental nickel magnetic moment in NiO and the theoretical value for the Ni^{2+} ion was taken as proof of electron localization. We would like to recall here that for a lot of other magnetic oxides, as for magnetite, the measured magnetic moment separates significantly from the theoretical ionic one. In our opinion, the agreement between the theoretical and experimental values of the magnetic moment in nickel oxide should be explained in more detail.

We will not consider in the following discussion the case of TM oxides with the formal integral valence state of the transition metal atom. We will deal with the formal mixed valence TM oxides and, in particular, the case of the archetypical compound magnetite, where the number of mobile electrons is one half of the number of lattice points. The key point is that atomic electronic localization in these mixed valence compounds implies necessarily spatial or temporal segregation into two ionic states. Taking as the reference magnetite, the description given by Verwey where Fe^{3+} and Fe^{2+} ions are ordered periodically on the B sites below T_V is an example of spatial localization while above T_V the charge fluctuates between the B sites giving an example of temporal localization. On the other hand, we have shown that from the experimental point of view neither ionic Fe^{3+}–Fe^{2+} ordering below T_V nor temporal localization above T_V has been found. Consequently, the insulator state below T_V cannot be associated with atomic electron localization and the Mott model for metal–insulator transitions does not apply to this system. In this sense, as the characteristic time for an x-ray absorption process is of the order of 10^{-16} s, the mixing of the electronic states between Fe atoms in the

lattice is very substantial. As a consequence, taking the atomic d orbitals as the basis functions for describing the electrical conduction in magnetite is not a good approach. In other words, speaking in terms of $3d^n$ configurations loses its meaning when the states are highly mixed in the solid. In this case, the energy of correlation between electrons on neighbouring atoms is important instead of the on-site Coulomb repulsion U.

A realistic calculation of the band structure of the high temperature phase of magnetite was made by the self-consistent APW method, using the local spin density approximation and taking into account the relativistic effects [151]. The band dispersion shows a large hybridization of Fe 3d states and O 2p states indicating the itinerant character of the electronic states. The Fermi level E_F lies within the energy gap of the majority spin band where the 3d levels of the Fe in the B site are almost occupied. In contrast, the 3d states of the Fe(B) site are almost empty in the minority spin band where the E_F is located. The total width of the valence band is about 10 eV below the Fermi level. Several experiments are consistent with this band structure. For example, the magnetic moment of a Fe atom on the A site is 3.82 μ_B, instead of 5 μ_B. Another important conclusion from this band structure [151] is that the difference of charges of Fe ions in the low temperature phase, or the amplitude of charge density waves, cannot be as large as 1 electron/Fe. Since the first band lies below the Fermi surface and will not be disturbed by the Verwey transition, all the Fe ions in the B sites always have at least $1/4$ of an electron. Consequently, the difference in valence of the Fe ions in the low temperature phase should be less than 0.5 e^-.

The insulating state of Fe_3O_4 has been analysed by means of local density approximation calculations including a Coulomb interaction correction [152, 153]. With the belief that the low temperature phase of magnetite is ordered, these supposed first-principles calculations include an effective inter-site Coulomb interaction (V). Even including this non-justified term V, they found a charge segregation of about 0.32 electrons, also far from the pure ionic value 1 [153]. In any case, we note that these calculations assume the charge ordering as a fact. It is clear that if we include some kind of interaction distinguishing near neighbour configurations, a charge ordered phase should be obtained. Recently, a self-interaction corrected local spin density calculation determined that the inequivalent Fe positions of the low temperature phase give rise to different charge distributions while the Fe valence remains unaltered [154]. Thus it was concluded that the charge disproportionation below the Verwey temperature is not of electronic origin but determined by structural distortions, and all the Fe ions occur in a trivalent state. This recent theoretical result agrees with the conclusion derived from diffraction experiments that the low temperature phase is characterized by at least four different Fe B atoms (perhaps 16) and the possible charge segregation has its origin in the existence of different crystallographic sites.

Many other models, based on the idea that the electron–phonon coupling leads to the formation of polarons in the low temperature phase, have also been proposed to describe the mechanism of electrical conduction and its behaviour near the Verwey transition in Fe_3O_4. We do not review these polaronic models proposed for magnetite here. We would merely like to remark that the time for hopping between Fe ions should be higher than 10^{-16} s and the characteristic time for thermal vibrations is lower than this value. So the electronic states coupled with phonons should be those extended over several atoms and not the localized ones. This fact excludes the possibility of the small polaronic models giving a realistic description of the electronic properties of magnetite.

6. Conclusions

Magnetite is a fascinating material that, despite being discovered more than 2000 years ago, is not yet well understood. The important fact is that magnetite has been taken as a reference

for all the solid state physics developed in the second half of the 20th century. In particular, the interpretation of the Verwey transition in terms of pure ionic ordering of the Fe ions at the octahedral B sites has been taken as a model for the theory of highly correlated electron systems and, in some way, as a basis of the Mott–Hubbard model. It seems more a sociological than a scientific problem that after 60 years from the proposal of the Verwey model, an important part of the scientific community continue to believe the Verwey description when the detailed scheme of charge order has not yet been determined.

As we have shown, there is no experimental proof supporting an atomic electronic localization in magnetite, and some of the experiments that claim to prove the CO model instead do the opposite. In particular, conventional x-ray diffraction, neutron diffraction and x-ray resonant scattering techniques demonstrate that there is no ionic ordering and, probably more important, no one-to-one charge segregation in magnetite below T_V (more than two different octahedral iron ions are present at low temperatures). In addition, the same conclusion applies to other related Fe and/or transition metal oxides, as we have discussed in section 4. This led us to reconsider the theories based on the model of an atomic localized character of the 3d electrons in transition metal oxides for describing the broad phenomenology of these compounds. For instance, high T_c superconductors and colossal magnetoresistive manganites are not yet well understood and, moreover, the present knowledge seems inadequate for predicting new properties of oxides. Thus, it seems that the atomic approach used to describe the physics of TM oxides needs to be modified and new ideas need to be developed in order to establish a coherent framework for explaining all the experimental data.

Acknowledgments

We would like to thank Drs J Blasco, M G Proietti, M C Sánchez, H Renevier and J L Hodeau for fruitful discussions and contributions to the x-ray resonant scattering experiments. This work was supported by the MCYT project No MAT2002-01221.

References

[1] Brandow B H 1977 *Adv. Phys.* **26** 651
[2] 1980 The Verwey transition *Phil. Mag.* **42** (special issue)
[3] Tsuda N, Nasu K, Yanase A and Siratori K 1990 *Electronic Conduction in Oxides* (Berlin: Springer)
[4] Honig J M 1985 Transitions in selected transition-metal oxides *The Metallic and Nonmetallic States of Matter* ed P P Edwards and C N R Rao (London: Taylor and Francis) p 261
[5] Brabers V A M 1995 Progress in spinel research *Handbook of Magnetic Materials* ed K H J Buschow (Amsterdam: Elsevier)
[6] Imada M 1998 Metal–insulator transitions *Rev. Mod. Phys.* **70** 1079
[7] Walz F 2002 *J. Phys.: Condens. Matter* **14** R285
[8] Goto T and Lüthi B 2003 *Adv. Phys.* **52** 67
[9] Néel L 1948 *Ann. Phys. Fr.* **3** 137
[10] Verwey E J W 1939 *Nature* **144** 327
[11] Verwey E J W and Haayman P W 1941 *Physica* **8** 979
[12] Verwey E J W, Haayman P W and Romeijn F C 1947 *J. Chem. Phys.* **15** 181
[13] Mott N F 1980 *Phil. Mag.* B **42** 327
[14] García J, Subías G, Proietti M G, Renevier H, Joly Y, Hodeau J L, Blasco J, Sánchez M C and Bérar J F 2000 *Phys. Rev. Lett.* **85** 578
[15] García J, Subías G, Proeitti M G, Blasco J, Renevier H, Hodeau J L and Joly Y 2001 *Phys. Rev.* B **63** 054110
[16] Anderson P W 1956 *Phys. Rev.* B **102** 1008
[17] Bragg W H 1915 *Phil. Mag.* **30** 305
[18] Bragg W H and Brown G B 1926 *Z. Kristallogr.* **82** 325
[19] Weiss P and Forrer R 1929 *Ann. Phys.* **12** 279
[20] Rakhecha V C and Satya Murphy N S 1978 *J. Phys. C: Solid State Phys.* **11** 4389

[21] Parks G S and Kelley K K 1926 *J. Phys. Chem.* **30** 47
[22] Okamura T 1932 *Sci. Rep. Tohoku Imp. Univ.* **21** 231
[23] Hamilton W C 1958 *Phys. Rev.* **110** 1050
[24] Mott N F 1990 *Metal–Insulator Transitions* 2nd edn (London: Taylor and Francis)
[25] Shirane G, Chikazumi S, Akimitsu J, Chiba K, Matsui M and Fujii Y 1975 *J. Phys. Soc. Japan* **39** 949
[26] Iizumi M, Koetzle T F, Shirane G, Chikazumi S, Matsui M and Todo S 1982 *Acta Crystallogr.* B **38** 2121
[27] Herbst J F 1991 *Rev. Mod. Phys.* **63** 819
[28] Stragier H, Cross J O, Rehr J J, Sorensen L B, Bouldin C E and Woicik J C 1992 *Phys. Rev. Lett.* **21** 3064
[29] Proietti M G, Renevier H, Hodeau J L, García J, Bérar J F and Wolfers P 1999 *Phys. Rev.* B **59** 5479
[30] Materlik G, Sparks C J and Fisher K (ed) 1994 *Resonant Anomalous X-Ray Scattering, Theory and Applications* (Amsterdam: Elsevier Science B.V.)
[31] Honig J M 1995 *J. Alloys Compounds* **229** 24
[32] Helwege K-H (ed) 1970 *Landolt–Börnstein New Series* Group III, vol 4b (Berlin: Springer) p 65
[33] Kakol Z 1990 *J. Solid State Chem.* **88** 104
[34] Matsui M, Todo S and Chikazumi S 1977 *J. Phys. Soc. Japan* **42** 1517
[35] Kuipers A J M and Brabers V A M 1979 *Phys. Rev.* B **20** 594
[36] Miles P A, Westphal W B and Hippel V A 1957 *Rev. Mod. Phys.* **29** 279
[37] Aragón R, Buttrey D, Shepherd J P and Honig J M 1985 *Phys. Rev.* B **31** 430
[38] Shepherd J P, Aragón R, Koenitzer J W and Honig J M 1985 *Phys. Rev.* B **32** 1818
[39] Aragón R and Honig J 1988 *Phys. Rev.* B **37** 209
[40] Aragón R, Gehring P M and Shapiro S M 1993 *Phys. Rev. Lett.* **70** 1635
[41] Whall T E, Yeung K K, Proykova and Brabers V A M 1984 *Phil. Mag.* B **50** 689
[42] Whall T E, Yeung K K, Proykova and Brabers V A M 1986 *Phil. Mag.* B **54** 505
Whall T E, Yeung K K, Proykova and Brabers V A M 1986 *Phil. Mag.* B **55** 535
[43] Tanaka M, Akimitsu J, Inada Y, Kimizuka N, Shindo I and Siratori K 1982 *Solid State Commun.* **44** 687
[44] Shepherd J P, Koetnizer J W, Aragón R, Spalek J and Honig J M 1991 *Phys. Rev.* B **43** 8461
[45] Srivastava C M, Srinivasan G and Nanadikar N G 1979 *Phys. Rev.* B **19** 499
[46] Loos J and Novák P 2002 *Phys. Rev.* B **66** 132403
[47] Lenge J, Kronmüller H and Walz F 1984 *J. Phys. Soc. Japan* **53** 1406
[48] Pan L S and Evans B J 1978 *J. Appl. Phys.* **49** 1458
[49] De Grave E, Persoons R M, Vandenberghe R E and Bakker P M A 1993 *Phys. Rev.* B **47** 5881
[50] Künding W and Hargrove R S 1969 *Solid State Commun.* **7** 223
[51] Rubinstein M and Forester D W 1971 *Solid State Commun.* **9** 1675
[52] Berry F J, Skinner S and Thomas M F 1998 *J. Phys.: Condens. Matter* **10** 215
[53] Mizoguchi M 1978 *J. Phys. Soc. Japan* **44** 1501
Mizoguchi M 1978 *J. Phys. Soc. Japan* **44** 1512
[54] Novak P, Stepankova H, Englich J, Kohout J and Brabers V A M 2000 *Phys. Rev.* B **61** 1256
[55] Mizoguchi M 2001 *J. Phys. Soc. Japan* **70** 2333
[56] McIntire N S and Zetaruk D G 1977 *Anal. Chem.* **49** 1521
[57] Cai Y Q, Ritter M, Weiss W and Bradshaw A M 1998 *Phys. Rev.* B **58** 5043
[58] Thole B T and van der Laan G 1988 *Phys. Rev.* B **38** 3158
[59] Crocombette J P, Pollack M, Jollet F, Thromat N and Gauitier-Soyer M 1995 *Phys. Rev.* B **52** 3143
[60] Colliex C, Manoubi T and Ortiz C 1991 *Phys. Rev.* B **44** 11402
[61] Tafto J and Kirvanek O L 1982 *Phys. Rev. Lett.* **48** 560
[62] Agui A, Saitoh Y, Yoshigoe A, Nakatani T, Matshushita T and Mizumaki M 2002 *Surf. Rev. Lett.* **9** 843
[63] Kuiper P, Searle B G, Duda L C, Wolf R M and van der Zaag P J 1997 *J. Electron Spectrosc. Relat. Phenom.* **86** 107
[64] Pellegrin E *et al* 1999 *Phys. Status Solidi* **215** 797
[65] Antonov V N, Harmon B N and Yaresko A N 2003 *Phys. Rev.* B **67** 024417
[66] Maruyama H, Harada I, Kobayashi K and Yamazaki H 1995 *Physica* B **208/209** 760
[67] de Groot F M F, Grioni M, Fuggle J C, Ghijsen J, Sawatzky G A and Petersen H 1989 *Phys. Rev.* B **40** 5715
[68] Ma Y, Johnson P D, Wassdahl N, Guo J, Skytt P, Nordgren J, Rubensson J E, Böske T and Eberhardt W 1993 *Phys. Rev.* B **48** 2109
[69] Schedel-Niedrig Th, Weiss W and Schlögl R 1995 *Phys. Rev.* B **52** 17449
[70] Wu Z Y, Gota S, Jollet F, Pollak M, Gautier-Soyer M and Natoli C R 1997 *Phys. Rev.* B **55** 2570
[71] Chainani A, Yokoya T, Morimoto T, Takahashi T and Todo S 1995 *Phys. Rev.* B **51** 17976
[72] Lad R J and Henrich V E 1989 *Phys. Rev.* B **39** 13478
[73] Park S K, Ishikawa T and Tokura Y 1998 *Phys. Rev.* B **58** 3717

[74] Park J-H, Tjeng L H, Allen J W, Metcalf P and Chen C T 1997 *Phys. Rev.* B **55** 12813
[75] Cai Y Q, Nakatsuji K, Ohno S, Iiomori T, Yamada M and Komori F 2002 *Surf. Rev. Lett.* **9** 907
[76] Shannon R D 1976 *Acta Crystallogr.* A **32** 751
[77] Zuo J M, Spence J C H and Petuskey W 1990 *Phys. Rev.* B **42** 8451
[78] Iizumi M and Shirane G 1975 *Solid State Commun.* **17** 433
[79] Yoshida J and Iida S 1977 *J. Phys. Soc. Japan* **42** 230
[80] Wright J P, Attfield J P and Radaelli P G 2001 *Phys. Rev. Lett.* **87** 266401
[81] Wright J P, Attfield J P and Radaelli P G 2002 *Phys. Rev.* B **66** 214422
[82] García J, Subías G, Blasco J and Proietti M G, unpublished
(García J, Subías G, Blasco J and Proietti M G 2002 *Preprint* cond-mat/0211407)
[83] Benfatto M, Solera J A, García J and Chaboy J 2002 *Chem. Phys.* **282** 441
[84] Toll J S 1956 *Phys. Rev.* **104** 1760
[85] García J, Sánchez M C, Subías G and Blasco J 2001 *J. Phys.: Condens. Matter* **13** 3243
[86] Brouder C 1990 *J. Phys.: Condens. Matter* **2** 701
[87] Dmitrienko V E 1983 *Acta Crystallogr.* A **39** 29
Dmitrienko V E 1984 *Acta Crystallogr.* A **40** 89
[88] Templeton D H and Templeton L K 1985 *Acta Crystallogr.* A **41** 133
Templeton D H and Templeton L K 1986 *Acta Crystallogr.* A **42** 478
[89] García J and Subías G 2003 *Phys. Rev.* B **68** 127101
[90] Filkestein K D, Shen Q and Shastri S 1992 *Phys. Rev. Lett.* **69** 1612
[91] Templeton D H and Templeton L K 1994 *Phys. Rev.* B **49** 14850
[92] Templeton D H 1998 *Acta Crystallogr.* A **54** 158
[93] Hagiwara K, Kanazawa M, Horie K, Kokubun J and Ishida K 1999 *J. Phys. Soc. Japan* **68** 1592
[94] Kanazawa M, Hagiwara K, Kokubun J and Ishida K 2002 *J. Phys. Soc. Japan* **71** 1765
[95] Sasaki S, Toyoda T, Konoike Y, Yamawaki K and Tanaka M 2001 *Nucl. Instrum. Methods Phys. Res.* A **467/468** 1084
[96] Toyoda T, Sasaki S and Tanaka M 1999 *Am. Mineral.* **84** 294
[97] Sasaki S, Toyoda T, Yamawaki K and Ohkubo K 1998 *J. Synchrotron Radiat.* **5** 920–2
[98] Subías G, García J, Proietti M G and Blasco J 1997 *Phys. Rev.* B **56** 8183
[99] García J, Sánchez M C, Blasco J, Subías G and Proietti M G 2001 *J. Phys.: Condens. Matter* **13** 3229
[100] Goodenough J B 1971 *Prog. Solid State Chem.* **5** 145
[101] Sakai Y, Kaneda K, Tsuda N and Tanaka M 1986 *J. Phys. Soc. Japan* **55** 3181
[102] Nagakawa Y, Inazumi M, Kimizuka N and Siratori K 1979 *J. Phys. Soc. Japan* **47** 1369
[103] Iida J, Tanaka M, Kito H and Akimitsu J 1990 *J. Phys. Soc. Japan* **59** 4190
[104] Tanaka M, Akimitsu J, Inada Y, Kimizuka N, Shindo I and Siratori K 1982 *Solid State Commun.* **44** 687
[105] Siratori K, Mori N, Takahashi H, Oomi G, Iida J, Tanaka M, Kishi M, Nagakawa Y and Kimizuka N 1990 *J. Phys. Soc. Japan* **59** 631
[106] Yamada Y, Kitsuda K, Nohdo S and Ikeda N 2000 *Phys. Rev.* B **62** 12167
[107] Ikeda N, Mori R, Kohn K, Misumaki M and Akao T 2002 *Ferroelectrics* **272** 309
[108] Lindén J, Karen P, Kjekshus A, Miettinen J, Pietari T and Karppinen M 1999 *Phys. Rev.* B **60** 15251
[109] Woodward P M and Karen P 2003 *Inorg. Chem.* **42** 1121
[110] Vogt T, Woodward P M, Karen P, Hunter B A, Henning P and Moodenbaugh A R 2000 *Phys. Rev. Lett.* **84** 2969
[111] Karen P, Woodward P M, Linden J, Vogt T, Studer A and Fisher P 2001 *Phys. Rev.* B **64** 214405
[112] Battle P D, Gibb T C and Lightfoot P 1990 *J. Solid State Chem.* **84** 271
[113] Coey J M D, Viret M and von Molnar S 1999 *Adv. Phys.* **48** 167
[114] Dagotto E, Hotta J and Moreo A 2001 *Phys. Rep.* **344** 1
[115] Salamon M B and Jaime M 2001 *Rev. Mod. Phys.* **73** 583
[116] Radaelli P G, Marezio M, Hwang H Y, Cheong S-W and Batlogg B 1995 *Phys. Rev. Lett.* **75** 4488
[117] Radaelli P G, Cox D E, Marezio M and Cheong S-W 1997 *Phys. Rev.* B **55** 3015
[118] Blasco J, García J, De Teresa J M, Ibarra M R, Perez J, Algarabel P A, Marquina C and Ritter C 1997 *J. Phys.: Condens. Matter* **9** 10321
[119] Chen C H, Cheong S-W and Hwang H Y 1997 *J. Appl. Phys.* **81** 4326
[120] Mori S, Chen C H and Cheong S-W 1998 *Phys. Rev. Lett.* **81** 3972
[121] Jirak Z, Damay F, Hervieu M, Martin C, Raveau B, André G and Boureé F 2000 *Phys. Rev.* B **61** 1181
[122] Kawano H, Kajimoto R, Yoshizawa H, Tomioka Y, Kuwohara H and Tokura Y 1997 *Phys. Rev. Lett.* **78** 4253
[123] Murakami Y, Kawada H, Kawata H, Tanaka M, Arima T, Moritomo Y and Tokura Y 1998 *Phys. Rev. Lett.* **80** 1932

[124] Murakami Y, Hill J P, Gibbs D, Blume M, Koyama I, Tanaka M, Kawata H, Arima T, Tokura Y, Hirota K and Endoh Y 1998 *Phys. Rev. Lett.* **81** 582
[125] Zimmermann M V, Hill J P, Gibbs D, Blume M, Casa D, Keimer B, Murakami Y, Kao C-C, Tomioka Y and Tokura Y 1999 *Phys. Rev. Lett.* **83** 4872
[126] Zimmermann M V, Nelson C S, Hill J P, Gibbs D, Blume M, Casa D, Keimer B, Murakami Y, Kao C-C, Ventaraman C, Gog T, Tomioka Y and Tokura Y 2001 *Phys. Rev.* B **64** 195133
[127] Nakamura K, Arima T, Nakazawa A, Wakabayashi Y and Murakami Y 1999 *Phys. Rev.* B **60** 2425
[128] Elfimov E S, Anisimov V I and Sawatzky G A 1999 *Phys. Rev. Lett.* **82** 4264
[129] Benfatto M, Joly Y and Natoli C R 1999 *Phys. Rev. Lett.* **82** 636
[130] Grenier S, Hill J P, Gibbs D, Thomas K J, Zimmermann M v, Nelson C S, Kiryukhin V, Tokura Y, Tomioka Y, Casa D, Gog T and Venkataram C, unpublished
(Grenier S, Hill J P, Gibbs D, Thomas K J, Zimmermann M v, Nelson C S, Kiryukhin V, Tokura Y, Tomioka Y, Casa D, Gog T and Venkataram C 2003 *Preprint* cond-mat/0305216v1)
[131] Zimmermann M v, Grenier S, Nelson C S, Hill J P, Gibbs D, Blume M, Casa D, Keimer B, Murakami Y, Kao C-C, Venkataraman C, Gog T, Tomioka Y and Tokura Y 2003 *Phys. Rev.* B **68** 127102
[132] LePage Y and Marezio M 1984 *J. Solid State Chem.* **53** 13
[133] Lüdecke J, Jobst A, Sammalen V S, Morré E, Geibel C and Krane H-G 1999 *Phys. Rev. Lett.* **82** 3633
[134] Alonso J A, Martínez-Lope M J, Casais M T, García-Muñoz J L and Fernández-Díaz M T 2000 *Phys. Rev.* B **61** 1756
[135] Nakao H, Ohwada K, Takesue N, Fujji Y, Isobe M, Ueda Y, Zimmermann M v, Hill J P, Gibbs D, Woicik J C, Koyama I and Murakami Y 2000 *Phys. Rev. Lett.* **85** 4349
[136] Grenier S, Toader A, Lorenzo J E, Joly Y, Grenier B, Ravy S, Regnault L P, Henry J Y, Jegoudez J and Revcolevschi A 2002 *Phys. Rev.* B **65** 180101
[137] Joly Y, Grenier S and Lorenzo J E 2003 *Phys. Rev.* B **68** 104412
[138] Staub U, Meijer G I, Fauth F, Allenspach R, Bednorz J G, Karpinski J, Kazakov S M, Paolasini L and d'Acapito F 2002 *Phys. Rev. Lett.* **88** 126402
[139] Woodward P M, Cox D E, Vogt T, Rao C N R and Cheetham A K 1999 *Chem. Mater.* **11** 3528
[140] Woodward P M, Cox D E, Moshopoulou E, Sleight A W and Moritomo S 2000 *Phys. Rev.* B **62** 844
[141] Sommerfeld A 1928 *Z. Phys.* **47** 1
[142] Bloch F 1929 *Z. Phys.* **57** 545
[143] Bethe H 1928 *Ann. Phys., Lpz.* **87** 55
[144] De Boer and Verwey E J W 1937 *Proc. Phys. Soc.* A **49** 59
[145] Mott N F 1937 *Proc. Phys. Soc.* A **49** 72
[146] Mott N F 1949 *Proc. Phys. Soc.* A **62** 416
[147] Hubbard J 1963 *Proc. Phys. Soc.* A **276** 238
[148] Hubbard J 1964 *Proc. Phys. Soc.* A **277** 237
[149] Hubbard J 1964 *Proc. Phys. Soc.* A **281** 401
[150] Zaanen J, Sawatzky G A and Allen J W 1985 *Phys. Rev. Lett.* **55** 418
[151] Yanase A and Siratori K 1984 *J. Phys. Soc. Japan* **53** 312
[152] Anisimov V I, Elfimov I S, Hamada N and Terakura K 1996 *Phys. Rev.* B **54** 4387
[153] Zhang Z and Satpathy S 1991 *Phys. Rev.* B **44** 13319
[154] Szotek S, Temmerman W M, Svane A, Petit L, Stocks G M and Winter H 2003 *Phys. Rev.* B **68** 054415
[155] Joly Y 2001 *Phys. Rev.* B **63** 125120